Textural signatures of sediment supply in gravel-bed rivers: Revisiting the armour ratio

Daniel Vázquez-Tarrío, Hervé Piégay, Rosana Menéndez-Duarte

Textural signatures of sediment supply in gravel-bed rivers: revisiting the armour ratio

Daniel Vázquez-Tarrío[1, 2], Hervé Piegay[3] and Rosana Menéndez-Duarte[1, 2]

[1] Department of Geology, University of Oviedo, c\ Jesús Arias de Velasco, s/n 33005 Oviedo, Spain. danielvazqueztarrio@gmail.com

[2] INDUROT, University of Oviedo, Campus de Mieres, s/n 33600 Mieres, Spain

[3] University of Lyon, CNRS UMR 5600 EVS, Site ENS, F-69342 Lyon, France

Abstract:

The surface of the streambed in gravel-bed rivers is commonly coarser than the underlying bed material. This surface coarsening, or 'armouring', is usually described by means of the ratio between surface and subsurface grain-size metrics (the 'armour ratio'). Such surface coarsening is typical of river reaches that are degrading due to a deficit in sediment supply (e.g. gravel-bed reaches below dams or lakes), but non-degrading gravel-bed streams may also exhibit some degree of armouring in relation to specific hydrological patterns. For instance, selective transport during the recession limbs of long lasting floods may coarsen the bed more significantly than flash floods. Consequently, regional differences in bed coarsening should exist, reflecting in turn the variability in sediment and water regimes. In this paper, we explore the trends linking armour ratios to sediment supply, taking into account the differences in hydrological context. We based our analysis on a large data set of bedload and grain size measurements from 49 natural gravel-bed streams and four flume experiments compiled from the scientific literature. Our main outcome documents how the balances between sediment yields and transport capacities have a quantifiable reflection on the armour ratios measured in the field: we report strong and statistically significant correlations between bedload fluxes and surface grain-size, and an asymptotic rise in armour ratios with the decline of sediment supply. Hydrological controls are also observed, but they are small compared to the signal related to sediment supply. Additionally, the trends observed in the field data are comparable to those previously documented in flume experiments with varying sediment feed. In this regard, different kinds of bedforms and particle arrangements have been commonly described with progressive reductions in sediment inputs and the subsequent coarsening of the streambed. Hence, armour ratios serve as a proxy for the general organization of the streambed of gravel-bed streams, and our results quantify this streambed adjustment to the dominant sediment supply regime.

Keywords: Gravel-bed rivers, Armour ratio, Sediment supply, Bedload

1. Introduction

A longstanding idea in fluvial geomorphology is that balances between sediment transport capacities, water discharge and sediment supply influence channel geometry (Parker et al., 2007; Parker, 2008), bed slope (e.g. Lane, 1955; Borland, 1960; Wilcock et al., 2009), streambed texture (Dietrich et al., 1989; Nelson et al., 2009; Venditti et al., 2017) and planform morphology (Church, 2006). Short-term fluctuations in sediment supply (e.g. hillslope processes, bank erosion, fine release from the bed after large floods) lead to local and temporary adjustments in streambed texture (e.g. Church et al., 1998; Clayton and Pitlick, 2008; Turowski et al., 2011) and channel morphology (Hassan and Zimmerman, 2012). In the long term, the balances between sediment and water yields seem to exert a conspicuous control on dominant channel styles (Montgomery and Buffington, 1997; Buffington, 2012) and river metamorphosis (Métivier and Barrier, 2012).

Seminal flume experiments by Dietrich et al. (1989), and early field observations (e.g. Gessler, 1967; Willets et al., 1988), reported how reductions in sediment supply tend to promote active channel narrowing, surface coarsening, bedload fining and transport rate decrease in gravel-bed rivers. Coarsening and fine sediment depletion in the riverbed is driven by a combination of winnowing during low flows (Gomez, 1983, 1993, 1994), infiltration of fine sediment (Marion and Fraccarollo, 1997; Curran and Waters, 2014; Berni et al., 2018) and kinematic sorting (Wilcock, 2001; Bacchi et al., 2014; Ferdowski et al., 2017) during bed load transport. Substantial subsequent work documents the influence of sediment inputs on the spatial and vertical patterns of grain size sorting (Nelson et al., 2009; 2010), the development of particle arrangements (e.g. Church et al., 1998; Venditti et al., 2017) and overall streambed mobility (Richards and Clifford, 1991; Pfeiffer and Finnegan, 2018).

According to all of the above, surface grain-size responds to decreases in bedload through the expansion of coarse fixed patches (Nelson et al., 2009; Yager et al., 2015), resulting in a general coarsening of the streambed (Dietrich et al., 1989). Hence, the degree of the latter may provide an idea of the dominant sediment supply conditions of a given river reach (Dietrich et al., 1989; Sklar et al., 2009; Venditti et al., 2017). For this reason, fluvial geomorphologists have often used the field observation of surface coarsening as a way to characterize streambed mobility and/or to diagnose the magnitude of bed degradation below dams, for example (see Rollet et al. 2013; Vázquez-Tarrio et al. 2019). However, disparities in the patterns of sediment supply variability (e.g. at the annual, seasonal, intra-flood scale) between different hydrological contexts complicate the interpretation of surface coarsening measured in the field and its application to river diagnosis. For instance, rivers experiencing long-lasting and sustained floods tend to exhaust fine sediment from the riverbed, which in turn enhances the degree of coarsening compared to the situation expected in streams with comparable sediment supplies, but submitted to flash floods (Laronne et al., 1994; Hassan et al. 2006). The hydrological regime is then a source of variability in the degree of surface coarsening that overlaps the signal related to the dominant sediment supply conditions. Moreover, sediment supply is difficult to quantify due to inherent complexities in bedload measurement (Pitlick et al., 2012); therefore, the field assessment of streambed response to sediment supply fluctuations is not easy.

In this paper, we build on these ideas in order to quantify the relative weight of sediment supply versus hydrological controls in governing surface armouring. To accomplish this, we based our analysis on a large compilation of grain-size measurements and bedload discharge information extracted from the scientific literature for 49 natural gravel-bed rivers and four flume experiments. We structured this analysis in two steps. First, we performed a wide review of the compiled grain-size data, from which metrics adequate for exploring the links between bed texture and sediment supply were identified. Then, we performed a meta-analysis of the compiled data (based on the metrics introduced in the review) in order to highlight the main trends in armour ratios, and their covariation with channel hydraulics and bedload fluxes. Understanding the linkages between streambed texture and sediment transport regime is a key question in fluvial geomorphology, river ecology, civil engineering and river restoration (Pfeiffer et al., 2017). Consequently, our analysis may have interesting implications for near-future research on gravel-bed rivers.

2. Compiled data

The dataset used in the present paper consists of grain-size and bedload measurements collected at 49 river sites (summarized in Table 1). An important amount of the compiled data derives from the extensive campaign of sediment transport measurements carried out on Idaho, Nevada (King et al., 2004), Colorado and Wyoming rivers (Ryan et al., 2002; 2005), which probably represents some of the best available datasets on bedload in gravel-bed rivers to date. These data have previously been presented and analysed in several papers (Ryan et al., 2002; 2005; King et al., 2004; Barry et al., 2004; Mueller et al., 2005; Muskatirovic, 2008; Pitlick et al., 2008). The remaining data come from comparable measurements in other gravel-bed streams (Milhous, 1973; Emmet and Seitz, 1974; Seitz, 1977; Jones and Seitz, 1980; Reid and Frostick, 1986; Lisle, 1986; 1989; Williams and Rosgen, 1986; Gomez, 1988; Kuhle, 1992; Lisle and Madej, 1992; Andrews, 1994; Reid et al., 1995; Madej and Ozaki, 1996; McLean et al., 1999; Almedej, 2002; Church and Hassan, 2002; Wilcock and Kenworthy, 2002; Erwin et al., 2011; Mueller and Pitlick, 2014).

Grain sizes (surface and substrate/subsurface) for each selected river were obtained from the graphical reading of grain-size curves extracted from the corresponding papers. When bed material was sampled at several locations or moments in the same river, we averaged the results to obtain a characteristic grain-size measure for each case study. Stream discharge information is available for 44 of the 49 selected case studies, together with width-averaged data on the main flow characteristics (velocity, active width). Using this information, we computed bed shear stress based on Rickenmann and Recking's (2011) fit to Ferguson's (2007) friction law (for more details see the supplementary files). We also compiled, for each case study, values for the representative channel-forming or dominant discharge (Table 2), which were derived from the information provided in the original papers about the bankfull discharge (in single-thread channels) or the ~1 to 2-year return period discharge (in multi-thread channels) (Table 2). Information on bedload discharges was also available (Table 1); in this regard, we acknowledge the great work of data compilation carried out by Recking (2010; 2013), who provided bedload information for these field sites as supporting files (ibid).

River/Reach	Source	Channel style	Slope	Surface D_{84} (mm)	Subsurface D_{84} (mm)	GSD measuring method		Flow width (m)	Flow depth (m)	Q (m^3/s)	Qb (g/s·m)	N	Sediment sampling method
						Surface	*Subsurface*						
Big Wood River	*King et al. (2004)*	Plane-bed	0.091	250	101	Pebble count and core sampling	Core sampling	12.8	0.4-1.1	6.0-30.9	0.0-336.4	100	HS 7.62 or 15.2 cm (0.25 mm mesh)
Blackmare Creek	*King et al. (2004)*	Plane-bed	0.03	220	97	Pebble count and core sampling	Core sampling	4.94-11.89	0.1-0.5	0.3-4.7	0.0-6.8	88	HS 7.62 or 15.2 cm (0.25 mm mesh)
Boise river	*King et al. (2004)*	Riffle and pool	0.0038	141	86	Pebble count	Core sampling	52.4-61.0	0.6-2.1	33.7-291.7	0.4-633.5	82	HS 7.62 or 15.2 cm (0.25 mm mesh)
Borgne d'Arolla	*Gomez (1988)*	Step-Pool	0.03	19	12	Contact sampling technique	10 kg-volumetric sampling	0.3-2.2	0.0-0.1	0.0-0.3	56.2-837.0	31	HS (7.6 cm), 0.5 mm mesh
Chulitnana River	*Williams and Rosgen (1989)*	Braided	0.0008	52	184	Pebble count (?)	Dredge sampling	98.5-309.0	1.7-3.6	212.0-7104.0	213.0-2590.0	43	HS (7.62 cm)
Clearwater River	*Jones and Seiz (1980)*	Riffle and pool	0.00037	70	70	Pebble count	Sieve analysis of dug material	125.0-149.0	3.4-46.3	288.0-3511.0	0.1-284.0	78	HS (7.6 and 15 cm
Dollar Creek	*King et al. (2004)*	Plane-bed	0.0146	145	83	Pebble count and core sampling	Core sampling	7.0-11.9	0.2-0.5	0.4-6.4	0.0-9.7	85	HS 7.62 or 15.2 cm (0.25 mm mesh)
East Fork San Juan	*Ryan et al. (2005)*	Braided	0.008	112	52	Pebble count	Barrel method	15.0-17.2	0.3-0.5	2.8-13.8		77	Wadable version of Elwha sampler, 102 × 203 mm
East Saint-Louis Creek	*Ryan et al. (2002)*	Step-Pool	0.058	142	23	Pebble count	Barrel method	2.8-3.0	0.1-0.4	0.1-1.24	0.0-21.2	109	HS (7.6 cm)
Fool Creek	*Ryan et al. (2002)*	Plane-bed	0.053	100	59	Pebble count	Barrel method	1.7-2.1	0.1-0.2	0.0-0.5	0.0-14.7	95	HS (7.6 cm)

River/Reach	Source	Channel style	Slope	Surface D_{84} (mm)	Subsurface D_{84} (mm)	GSD measuring method		Flow width (m)	Flow depth (m)	Q (m^3/s)	Qb (g/s·m)	N	Sediment sampling method
						Surface	***Subsurface***						
Fraser River	*McLean et al. (1999); Ferguson and Church (2009)*	Riffle and pool	0.00046	70	68	Pebble count	Bulk volume sampling	510	-	1085-11445	0.3-486.3	76	Basket sampler (610 × 255 mm) for high flows and half- size VuV sampler (225 × 115 mm) for lower flows
Goodwin Creek	*Kuhnle (1992); Almedeij (2002)*	Riffle and pool	0.0021	30	30	Pebble count	Bulk volume sampling	11.1-14.6	0.4-1.2	1.4-21.6	0.2-2980.0	357	HS (58 cm2 with trapezoidal shape), 0.25mm net mesh
Harris Creek	*Church and Hassan (2002)*	Riffle and pool	0.013	100	55	Pebble count (grid-by-number)	Bulk mas sampling	15	-	4.2-18.4	0.0-4.3	22	Sediment trap
Jacoby	*Lisle (1986); Lisle (1989); Almadeij (2002); Wilcock and Kenworthy (2002)*	Riffle and pool	0.0063	95	81	Pebble count	Frozen core method	17.2	-	0.6-18.51	0.0-413.0	100	HS (4.4 cm)
Johns Creek	*King et al. (2004)*	Step-Pool	0.0207	558	63	Pebble count	Core sampling	8.2-14.6	0.3-1.2	1.0-34.3	0.0-10.7	46	HS 7.62 or 15.2 cm (0.25 mm mesh)
Little Buckhorn Creek	*King et al. (2004)*	Step-Pool	0.0509	340	94	Pebble count and core sampling	Core sampling	1.4-4.6	0.1-0.7	0.1-0.7	0.0-18.5	78	HS 7.62 or 15.2 cm (0.25 mm mesh)

River/Reach	Source	Channel style	Slope	Surface D_{84} (mm)	Subsurface D_{84} (mm)	GSD measuring method		Flow width (m)	Flow depth (m)	Q (m^3/s)	Qb (g/s·m)	N	Sediment sampling method
						Surface	*Subsurface*						
Little Granite Creek	*Ryan et al. (2002)*	Plane-bed	0.019	220	41	Pebble count	Barrel method	6.5-11.2	-	0.7-11.6	0.0-128.0	123	HS (7.6 cm)
Little Slate	*King et al. (2004)*	Plane-bed	0.0268	380	141	Pebble count and core sampling	Core sampling	6.7-13.4	0.3-1.0	0.5-18.3	0.0-10.3	157	HS 7.62 or 15.2 cm (0.25 mm mesh)
Lochsa Creek	*King et al. (2004)*	Plane-bed	0.0023	245	123	Pebble count and core sampling	Core sampling	67.1-83.0	1.8-3.1	110.7-758.9	0.0-48.3	72	HS 7.62 or 15.2 cm (0.25 mm mesh))
Lolo Creek	*King et al. (2004)*	Plane-bed	0.0097	140	68	Pebble count and core sampling	Core sampling	10.7-16.0	0.3-1.5	1.8-23.0	0.0-13.4	89	HS 7.62 or 15.2 cm (0.25 mm mesh)
Middle Fork	*King et al. (2004)*	Plane-bed	0.0041	288	140	Pebble count and core sampling	Core sampling	42.7-67.1	1.2-2.01	83.5-433.2	0.1-727.7	64	HS 7.62 or 15.2 cm (0.25 mm mesh)
Middle Fork Piedra River	*King et al. (2004)*	Riffle and pool	0.011	210	43.3	Pebble count and core sampling	Core sampling	11.4-13.8	0.2-0.5	1-11.0	0.0-216.6	86	HS 7.62 or 15.2 cm (0.25 mm mesh)
Nahal Yatir	*Reid et al. (1995)*	Riffle and pool	0.0088	13	34	Removing clasts from spray-painted stripes and laboratory sieving	Bulk volume sampling	3.5	0.1-0.6	0.3-0.5	200.0-7050.0	74	Sediment trap
North Fork Clearwater	*King et al. (2004)*	Plane-bed	0.0005	270	104	Pebble count and core sampling	Core sampling	9.1-93.6	1.7-34.1	100.8-974.1	0.0-732.2	72	HS 7.62 or 15.2 cm (0.25 mm mesh)
Oak Creek	*Milhous (1973)*	Plane-bed	0.0083	80	52	Pebble count and bottom samplers	Bulk volume sampling	3.7	-	0.0-3.4	0.0-111.0	119	Sediment trap, vortex tube

River/Reach	Source	Channel style	Slope	Surface D_{84} (mm)	Subsurface D_{84} (mm)	GSD measuring method		Flow width (m)	Flow depth (m)	Q (m^3/s)	Qb (g/s·m)	N	Sediment sampling method
						Surface	***Subsurface***						
Pacific creek	*Erwin et al. (2011)*	Braided	0.0035	45	28	Pebble count	Bulk volume sampling	-	-	-	-	-	-
Rapid River	*King et al. (2004)*	Plane-bed	0.0108	170	101	Pebble count	Core sampling	11.4-18.6	0.2-0.9	0.9-36.8	0.0-294.3	190	HS 7.62 or 15.2 cm (0.25 mm mesh)
Redwood Creek	*Lisle and Madej (1992); Madej and Ozaki (1996)*	Riffle and pool	0.0014	18	20	Pebble count	Bulk volume sampling	11.7-70	-	1.8-569	8.1-5067.8	221	HS sampler (7.6 cm)
Saint-Louis Creek	*Ryan et al. (2002; 2005)*	Plane-bed	0.0110-0.0450	162-543	33-78	Pebble count	Barrel method	5.2-10.3	0.1-0.4	0.4-7.2	0.0-65.7	813	HS (7.6 cm)
Sagehen Creek	*Andrews (1994)*	Riffle and pool	0.0102	104	96	Pebble count	Bulk volume sampling	2.6	0.3-1.6	1.0-3.1	0.5-34.9	55	HS (15 cm)
Salmon River below Yankee	*King et al. (2004)*	Plane-bed	0.0034	276	99	Pebble count and core sampling	Core sampling	30.5-38.4	1.2-1.9	38.5-143.6	0.0-98.8	60	HS 7.62 or 15.2 cm (0.25 mm mesh)
Salmon River near Obsidian	*King et al. (2004)*	Plane-bed	0.0066	128	84	Pebble count and core sampling	Core sampling	12.0-14.3	0.7-0.9	7.5-21.0	0.7-103.4	50	HS 7.62 or 15.2 cm (0.25 mm mesh)
Salmon River near Shoup	*King et al. (2004)*	Plane-bed	0.0019	174	136	Pebble count and core sampling	Core sampling	46.5-99.5	1.7-2.7	108.4-540.8	1.0-536.1	60	HS 7.62 or 15.2 cm (0.25 mm mesh)
Selway River	*King et al. (2004)*	Plane-bed	0.0021	265	173	Pebble count and core sampling	Core sampling	82.3-97.8	1.4-2.8	134.8-1067.5	0.0-43.5	72	HS 7.62 or 15.2 cm (0.25 mm mesh)

River/Reach	Source	Channel style	Slope	Surface D_{84} (mm)	Subsurface D_{84} (mm)	GSD measuring method		Flow width (m)	Flow depth (m)	Q (m^3/s)	Qb (g/s·m)	N	Sediment sampling method
						Surface	*Subsurface*						
Silver Creek	*Ryan et al. (2005)*	Plane-bed	0.0450	73	33	Pebble count	Barrel method	3.8-4.4	0.1-0.3	0.1-1.4	0.0-214.3	57	Wadable version of the Elwha sampler, 102 × 203 mm
Snake River	*Emmett and Seitz (1974);Seitz (1977)*	Riffle and pool	0.0009	115	54	Pebble count	Sieve analysis of dug material	155.4-204.2	3.3-6.2	779.0-4559.0	0.0-342.0	63	HS (7.6 and 15 cm)
Snake River below Jackson Lake	*Mueller and Pitlick (2014)*	Braided	0.0025	83	58	Pebble count	Bulk volume sampling	-	-	-	-	-	-
South Fork Payette	*King et al. (2004)*	Plane-bed	0.004	150	79	Pebble count and core sampling	Core sampling	43.6-51.8	0.4-1.7	20.4-180.9	-	-	HS 7.62 or 15.2 cm (0.25 mm mesh)
South Fork Red River	*King et al. (2004)*	Plane-bed	0.0146	150	161	Pebble count and core sampling	Core sampling	5.8-12.2	0.1-0.9	0.2-13.0	0.0-29.0	204	HS 7.62 or 15.2 cm (0.25 mm mesh)
Squaw Creek USGS	*King et al. (2004)*	Plane-bed	0.01	72	93	Pebble count and core sampling	Core sampling	3.3-14.1	0.2-0.4	0.1-7.6	0.0-23.0	92	HS 7.62 or 15.2 cm (0.25 mm mesh)
Sunlight Creek-4	*Mueller and Pitlick (2014)*	Braided	0.0075	94.6	43	Pebble count	Bulk volume sampling	-	-	-	-	-	-
Sunlight Creek-11	*Mueller and Pitlick (2014)*	Riffle and Pool	0.0091	79.2	55	Pebble count	Bulk volume sampling	-	-	-	-	-	-
Susitna River near Talkeetns	*Williams and Rosgen (1986)*	Braided	0.0015	96	260	Pebble count, bulk sampling (?)	Bulk sampling (?), dredge sampling	118.0-202.0	1.1-14.0	240.0-1310.0	0.9-156.0	39	HS (7.62 cm)

River/Reach	Source	Channel style	Slope	Surface D_{84} (mm)	Subsurface D_{84} (mm)	GSD measuring method		Flow width (m)	Flow depth (m)	Q (m^3/s)	Qb (g/s·m)	N	Sediment sampling method
						Surface	***Subsurface***						
Susitna River at Sunshine, Alaska	*Williams and Rosgen (1986)*	Braided	0.0017	88	163	Pebble count, bulk sampling (?)	Bulk sampling (?), dredge sampling	174.0-311.0	2.1-4.4	504.0-2800.0	33.7-1500.0	41	HS (7.62 cm)
Talkeetna River near Talkeetna	*Williams and Rosgen (1986)*	Braided	0.00096	100	184	Bulk sampling (?)	Bulk sampling (?) dredge sampling	-	-	-	-	-	-
Thompson Creek	*King et al. (2004)*	Plane-bed	0.0153	110	132	Pebble count and core sampling	Core sampling	4.2-6.7	0.2-0.4	0.2-3.5	0.0-38.0	84	HS 7.62 or 15.2 cm (0.25 mm mesh)
Trapper Creek	*King et al. (2004)*	Step-Pool	0.0414	122	67	Pebble count and core sampling	Core sampling	3.5-6.4	0.1-0.6	0.1-3.8	0.0-31.3	166	HS 7.62 or 15.2 cm (0.25 mm mesh)
Turkey Brook	*Reid and Frostick (1986)*	Riffle and pool	0.0142	42	35	No information	No information	3	0.1-0.9	0.1-13.8	0.0-50.6	206	Pit traps
Valley Creek	*King et al. (2004)*	Plane-bed	0.0040	160	78	Pebble count and core sampling	Core sampling	17.7-42.3	0.4-1.3	3.9-40.2	0.0-56.8	192	HS 7.62 or 15.2 cm (0.25 mm mesh)

Table 1. Sources of field data and information compiled for this study. D_{84}: 84-th percentile of the grain-size distribution (GSD). *Q*: Flow discharges. *Qb*: Bedload discharges. *HS*: Helley-Smith sampler. *N*: number of data.

River/Reach	Dominant discharge (m^3/s)	Flow recurrence (years)	River/Reach	Dominant discharge (m^3/s)	Flow recurrence (years)	River/Reach	Dominant discharge (m^3/s)	Flow recurrence (years)	River/Reach	Dominant discharge (m^3/s)	Flow recurrence (years)
Big Wood River	21.7	1.5	Harris creek	19.0	1	Oak Creek	3.4***	No info	Snake River below Jackson Lake	285**	1.5 - 2
Blackmare Creek	4.7*	1.1	Jacoby	19.6	No info	Rapid river	17.7*	1.4	South Fork Payette	86.4*	1.2
Boise river	167.1*	1.7	Johns creek	49.0*	3.4	Pacific creek	60.1	1.5 - 2	South Fork Red River	7.3*	1.5
Borgne d'Arolla	0.2*	< 1	Little Buckhorn Creek	0.2	1	Redwood Creek	560*	2 – 5	Squaw Creek USGS	5.1*	1.6
Chulitnana River	1130**	2	Little Granite Creek	5.9*	1.5	Saint-Louis Creek	2.6 – 4.8*	1.5	Sunlight Creek-4	16.5**	1.5 - 2
Clearwater River	2662***	2.2 - 2.3	Little Slate	12.2*	1.4	Sagehen Creek	2	~ 1	Sunlight Creek-11	14**	1.5 - 2
Dollar Creek	6.4*	1.1	Lochsa Creek	446*	1.5	Salmon River below Yankee	118.1	1.5	Susitna River near Talkeetns	1270**	2
East Fork San Juan	15.7*	1.5	Lolo Creek	11.8*	1.2	Salmon River near Obsidian	12.5	1.5	Susitna River at Sunshine, Alaska	4020**	2
East Saint-Louis Creek	0.9*	1.5	Middle Fork	217	1.5	Salmon River near Shoup	320	1.5	Talkeetna River near Talkeetna	730**	2
Fool Creek	0.3*	1.5	Middle Fork Piedra River	10.1*	1.5	Selway River	651.3*	1.7	Thompson Creek	2.5*	1.6
Fraser River	8760	1	Nahal Yatir	7.9	No info	Silver Creek	1.3*	1.5	Trapper Creek	2.6*	1.9
Goodwin creek	10.6	No info	North Fork Clearwater	453.1*	1.5	Snake River	3426***	2.2 – 2.3	Turkey Brook	19.6	No info
									Valley Creek	24.1*	1.6

Table 2. Information on the dominant channel-forming discharge for the case study selected for the present meta-analysis. (*) Bankfull discharge. (**) Dominant discharge provided by Mueller and Pitlick (2014). (***) Reference discharge provided by Church and Rood (1983)

River/Reach	Sediment supply	Flow regime	River/Reach	Sediment supply	Flow regime	River/Reach	Sediment supply	Flow regime	River/Reach	Sediment supply	Flow regime
Big Wood River	Moderate	Snowmelt	Harris creek	Low	Rain-on-snow/Snowmelt	Oak Creek	Low	Rainfall	Snake River below Jackson Lake	High	-
Blackmare Creek	Low	Snowmelt	Jacoby	Low	Rainfall	Pacific creek	High	Rainfall	South Fork Payette	Low/Moderate	Snowmelt
Boise river	Moderate /High	Snowmelt	Johns creek	Low	Snowmelt	Rapid river	Moderate	Rain-on-snow/Snowmelt	South Fork Red River	Low	Snowmelt
Borgne d'Arolla	High	Glacial fed	Little Buckhorn Creek	Low	Snowmelt	Redwood Creek	High	Rainfall	Squaw Creek USGS	Moderate	Snowmelt
Chulitnana River	High	Glacial fed	Little Granite Creek	Low /Moderate	Snowmelt	Saint-Louis Creek	Low	Snowmelt	Sunlight Creek-4	High	Snowmelr
Clearwater River	Moderate /High	Impounded	Little Slate	Low	Snowmelt	Sagehen Creek	Low	Snowmelt	Sunlight Creek-11	Moderate/ High	Snowmelt
Dollar Creek	Low	Snowmelt	Lochsa Creek	Moderate	Rain-on-snow/Snowmelt	Salmon River below Yankee	Low/Moderate	Snowmelt	Susitna River near Talkeetns	High	Glacial fed
East Fork San Juan	High	Rain-on-snow/Snowmelt	Lolo Creek	Low/Moderate	Snowmelt	Salmon River near Obsidian	Moderate/High	Snowmelt	Susitna River at Sunshine, Alaska	High	Glacial fed
East Saint-Louis Creek	Low	Snowmelt	Middle Fork	Moderate/High	Snowmelt	Salmon River near Shoup	Moderate	Snowmelt	Talkeetna River near Talkeetna	High	Glacial fed
Fool Creek	Low	Snowmelt	Middle Fork Piedra River	Low	Rain-on-snow/Snowmelt	Selway River	Moderate	Rain-on-snow/Snowmelt	Thompson Creek	Moderate	Snowmelt
Fraser River	High	Snowmelt	Nahal Yatir	High	Flash-floods	Silver Creek	Moderate	Rain-on-snow/Snowmelt	Trapper Creek	Low	Snowmelt
Goodwin creek	Moderate	Rainfall	North Fork Clearwater	Moderate	Rain-on-snow/Snowmelt	Snake River	Moderate/High	Impounded	Turkey Brook	Low	Flahs-floods
									Valley Creek	Moderate	Snowmelt

Table 3. Information on sediment-supply at the catchment scale and dominant flow regime for the data compiled in the present work.

We grouped the data following three different criteria. We made an initial classification according to dominant channel morphology, grouping the different case studies as riffle and pool, step-pool and plane-bed channels (after Montgomery and Buffington, 1997). Due to its geomorphological significance, we also defined a separate group for multi-thread rivers, in spite of the fact that each single thread of a braided river commonly shows a riffle and pool or bar-pool morphology. We also classified the different data according to the general sediment supply conditions at the catchment scale (Table 3). Following Recking (2012), we defined three main groups of data: i. low sediment supply, with channels draining highly vegetated watersheds and no clear active sediment sources and/or alluvial material; ii. moderate sediment supply, with rivers located in catchments in which significant bare land areas and/or sparse vegetation, and punctually distributed active sediment sources, are observed; and iii. high sediment supply, with channels well-coupled to landslides/slope deposits, or fed by strong bank erosion and/or bar-edge trimming (e.g. channels with braided morphology). We based this classification on the scarce information (study site description, photographs, etc.) provided by the original studies and our own inspection of the rivers through Google Earth. Finally, we also grouped the compiled data according to dominant flow regime, differentiating between: i. 'rainfall-dominated'; ii. 'snowmelt/rain-on-snow-dominated'; iii. 'snowmelt-dominated'; iv. 'glacial-fed' and v. 'flash-flood dominated' streams (Table 3).

Flume	Source	S	W (m)	L (m)	h (cm)	D_{50s} (mm)	Shields	Feed rate	r (h)
Tsukuba	*Nelson et al. (2009)*	0.0035-0.0052	7.5	0.3	10.2-11.3	3.7-4.9	0.049-0.086	1.7-17.4g/min·cm	6-7.5
Berkeley	*Nelson et al. (2009)*	0.0043-0.0055	28	0.9	21.8-22.8	10.1-11.8	0.045-0.061	0-23.3 g/min·cm	20.7-28.9
UBC	*Church et al. (1998)*	0.001-0.012	0.5/0.8	6/10	0.5-7.4	1.9-5.1	0.003-0.117	No feed	-
UBC	*Hassan and Church (200)*	0.006/0.007	0.8	10	0.1-6.7	2.4-4.5	-	1.2-0.644 kg/h	96

Table 4. Sources of flume data compiled for this study. *S:* Flume slope. *W*: Flume width. *L*: Flume length. *h*: water depth. D_{50}: 50-th percentile of sediment GSD. *r*: experiment duration.

Apart from field data, we also benefited from the results of previous flume experiments that explored the role of sediment feed reductions on the surface texture (Church et al., 1998; Hassan and Church, 2000; Nelson et al., 2009). Table 4 describes the main characteristics of these experiments. Information for these flume investigations was extracted from graphical reading of figures presented in Venditti et al. (2017) (Figures 16.1, 16.2 and 16.5 in that paper).

3. Review of the compiled data

3.1. Surface coarsening in gravel-bed rivers: introducing the 'armour ratio'

Streambed surface is, in general, coarser than the underlying subsurface grain-size distribution (GSD) in the compiled dataset: the average D_{50} and D_{84} are both coarser on the surface than the subsurface GSD (Figure 1A). The degree of surface coarsening has usually been quantified in fluvial geomorphology through the 'armour ratio' (D^*): the ratio between a characteristic grain size (normally, the median size) on the surface GSD and the same characteristic grain size in the subsurface GSD (Bunte and Abt, 2001):

$$D_i^* = \frac{D_{i_s}}{D_{i_{ss}}} \qquad \text{Eq. 1}$$

where D_i refers to the *i*th-percentile of the GSD. A value of D^* equal to 1 means that the surface and subsurface GSD are very similar. When the surface is coarser than the subsurface GSD, then $D^* > 1$; the coarser the surface is compared to the subsurface GSD, the larger the D^*. Average armour ratios are larger in the compiled data if estimated using the median size rather than using the D_{84} (~3.1 against ~1.8, respectively) (Figure 2), outlining that differences between both GSD are more important towards finer size fractions. In addition, some different tendencies could be appreciated according to channel morphology (Figure 3).

Apart from surface coarsening, some other complementary trends can be identified and seem intimately related to the former (Figures 1C and 1D). For instance, the percentages of fine sediment are, on average, larger in the subsurface (~15%) than on the surface GSD (~6%) (Figure 1D). Furthermore, patterns of grain-size sorting also show differences: D_{84}/D_{50} sorting indexes are again larger in the subsurface (~3.6 on average) than on the surface GSD (~2.1 on average), suggesting that subsurface GSD is more poorly sorted (Figure 1C). All these differences are statistically significant (Welch's t-test for unequal variances, p-value<0.05).

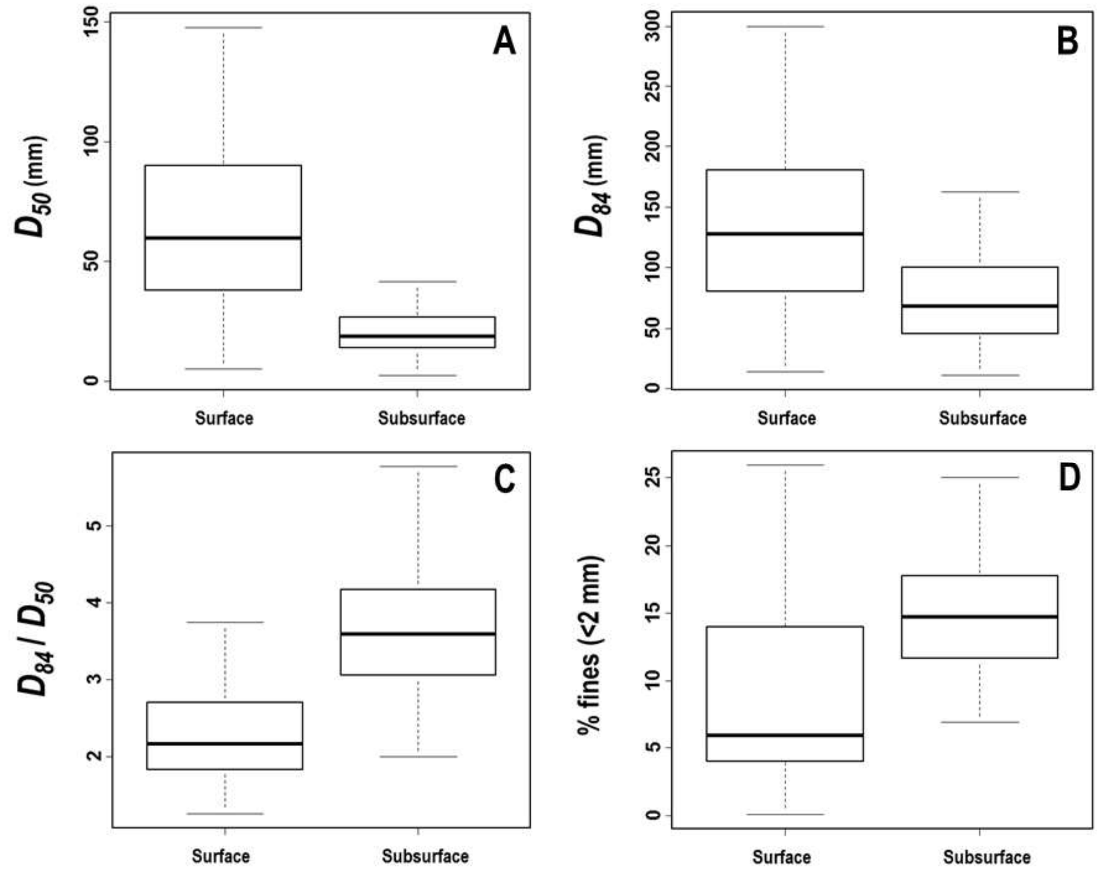

Figure 1. Comparison between surface and subsurface grain-size parameters in the compiled database. A: D_{50} (in mm); B: D_{84} (in mm). C: D_{84}/D_{50} ratio. D: Percentage of fines (< 2mm) present in the sediment.

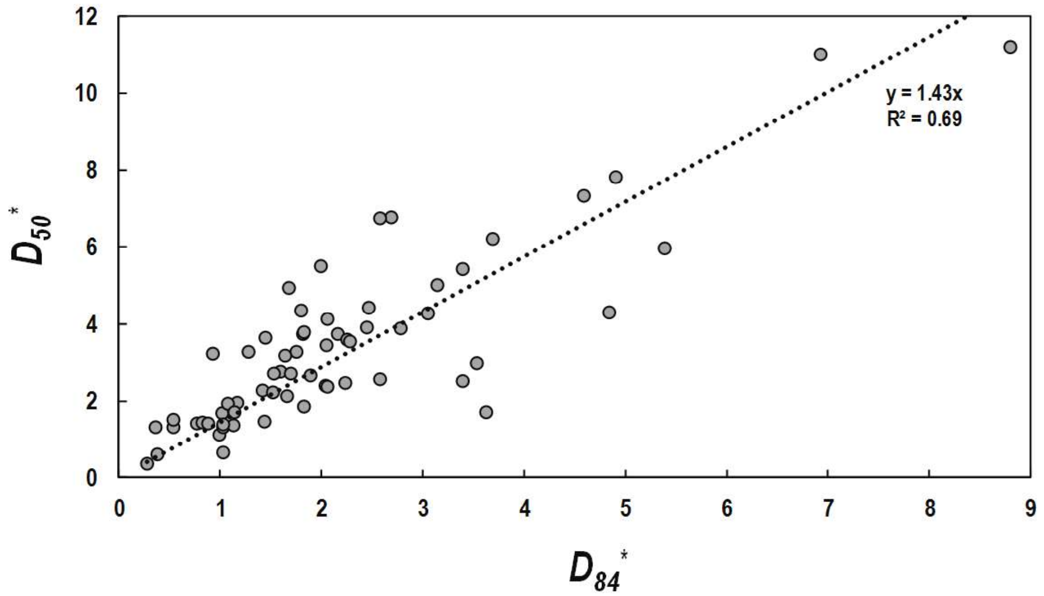

Figure 2. Armour ratios based on D_{50} plotted versus the armour ratios based on D_{84}.

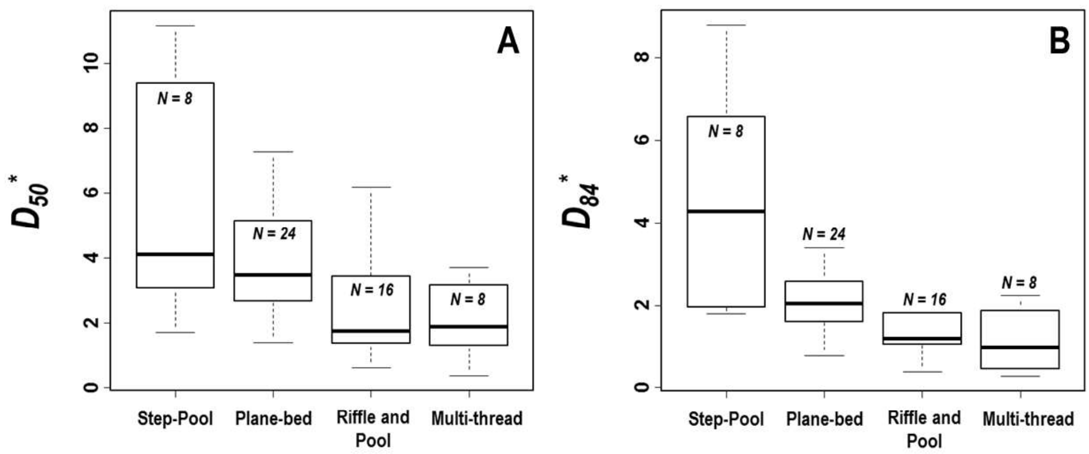

Figure 3. Differences in armour ratios according to channel morphology. A: Armour ratio based on the media size of the bed sediment (D_{50}). B: Armour ratio based on the 84-th percentile (D_{84}) of the grain-size distribution (GSD). N: Number of data.

It could initially be thought that methodological biases may explain a part of these trends. Subsurface GSD is commonly determined by sieving dredged or excavated bulk volume samples (Church et al., 1987). Conversely, a wide diversity of methods have been proposed to approach the surface GSD, such as the classical Wolman (1954) pebble-count method, the photosieving approach (Ibbeken and Schleyer, 1986, Butler et al., 2001, Rubin, 2004, Graham et al., 2005, Buscombe, 2008, Detert and Weitbrecht, 2013) or the more recent protocols based on high-resolution topography (e.g. Heritage and Milan, 2009; Brasington et al., 2012; Vázquez-Tarrío et al., 2017; Woodget et al., 2017). Grain sizes determined from area-by-weight sample methods (like the photosieving approach) are not directly equivalent to grain sizes determined from volume-by-weight sampling procedures (e.g. size sieving of bulk volume samples) (Kellerhals and Bray, 1971; Bunte and Abt, 2001). However, in the study cases compiled here, surface GSD was generally sampled using a grid-by-number pebble count, while subsurface GSD was always obtained from one variant or another (dredging, digging, frozen cores…) of the bulk volume sampling strategy (Table 1). Particle-size distributions determined from volume-by-weight (size-sieving of bulk volume samples) and grid-by-number (pebble count) samples are said to be equivalent (Kellerhals and Bray, 1971; Bunte and Abt, 2001; Rice and Haschenburger, 2004), and so surface coarsening seems to be a real trend in the compiled data, and not an artefact issuing from methodological biases.

3.2. Sediment supply vs. hydrologic controls on surface coarsening and 'armour ratios'

The grain size of sediment inputs should exert an obvious control on the grain calibre of the available bed material within a specific river reach, which in turn may condition the sediment size of the streambed's surface. In this regard, we could consider subsurface GSD as a proxy for the GSD of the average annual sediment inputs (Kuhnle and Willis, 1992; Lisle, 1995; Church and Hassan, 2005; Recking, 2013; Segura and Pitlick, 2015), i.e. the GSD available in the subsurface should condition the GSD of the streambed surface. Within the compiled data, we observe some statistically significant and moderate correlation between surface and subsurface GSD (Figure 4), which highlights this undeniable influence of the sediment supply GSD on the GSD of the streambed's surface. However, it is interesting to notice how variance in grain-size data is larger for surface than subsurface GSD (see Figures 1A and B). This suggests that grain-size variability introduced by the sediment supplies is diluted by the variability in surface coarsening introduced by some other controls.

In this regard, the compiled data show some statistically significant differences (ANOVA test, p-value < 0.05) in armour ratios according to the amounts of sediment supply at the catchment scale (Figure 5): rivers with high sediment supplies tend to show lower armour ratios than streams with low sediment feeds. Surface coarsening (often named 'armouring') has been described in gravel-bed settings for a long time (e.g. Gessler, 1967), and already related to the higher or lower availability of upstream sediment inputs. Armouring has been, thereby, typically reported in degrading beds and river reaches with low or no sediment supply (e.g. gravel-bed reaches below dams or lakes) (Gessler, 1967; Willets et al., 1988; Chin et al., 1994; Gomez, 1994; Vericat et al., 2006). In such cases, armouring is called 'static' or 'pavement' (Jain, 1990; Yager et al., 2015; Bertin and Freidrich, 2018). Static armours can 'break up' during high peaks of flow and/or transport episodes with large sand sediment supplies (Laronne and Carson, 1976; Gomez, 1983; Klaasen, 1988; Chin et al., 1994; Venditti et al., 2005; Vericat et al., 2006; Wang and Liu, 2009; Venditti et al., 2010; Spiller et al., 2012; Curran and Waters, 2014; Orrú et al., 2016; Bertin and

Freidrich, 2018) and re-form during the falling limb of the flood hydrograph, together with a progressive reduction in sediment mobility and the winnowing of finer and more mobile particles (Mao, 2012).

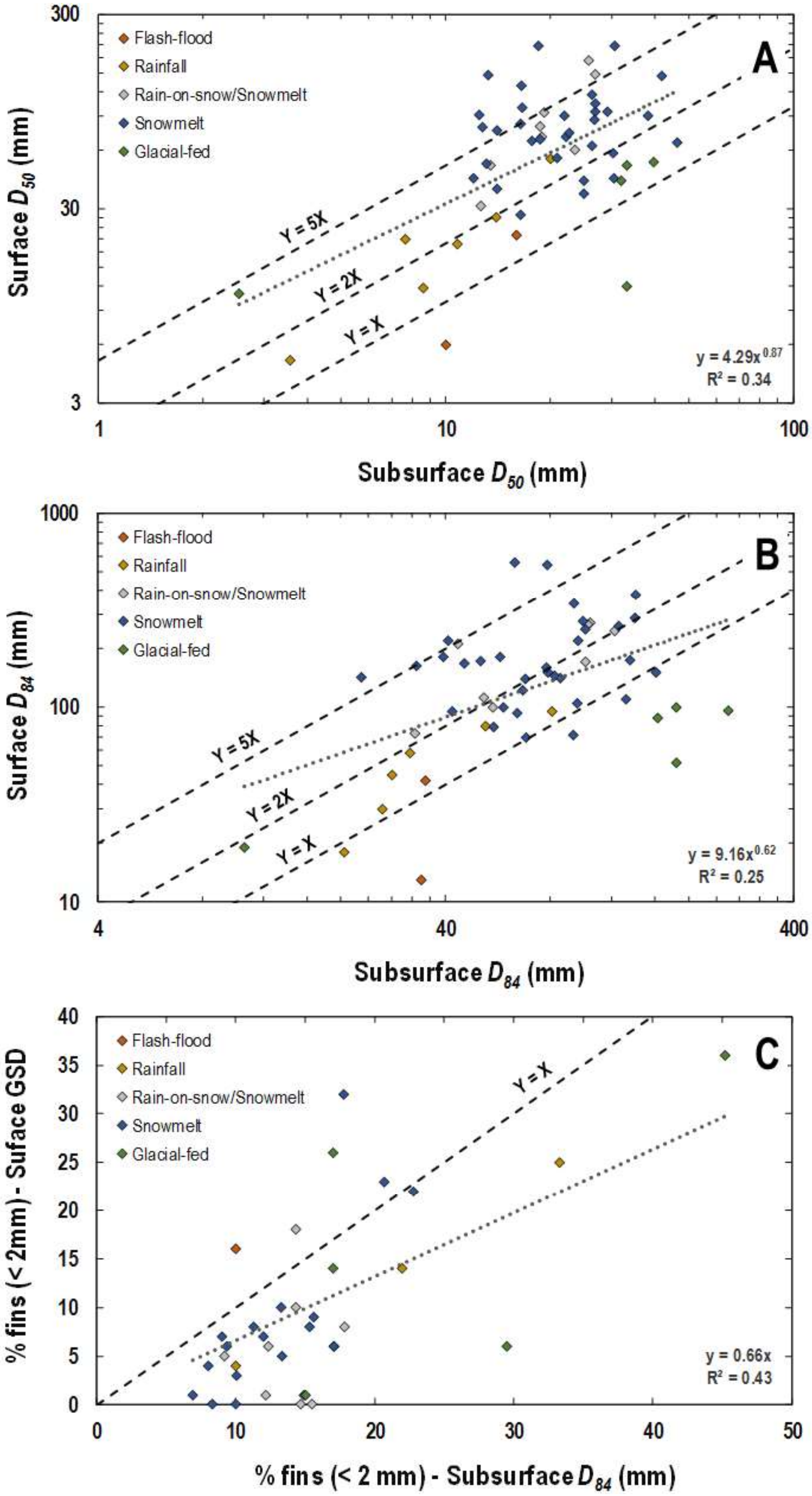

Figure 4. Surface grain-size parameters plotted versus subsurface parameters. A: D_{50}. B: D_{84}. C: Percentage of fine sediment (< 2 mm). We have segregated the data according to hydrological regime.

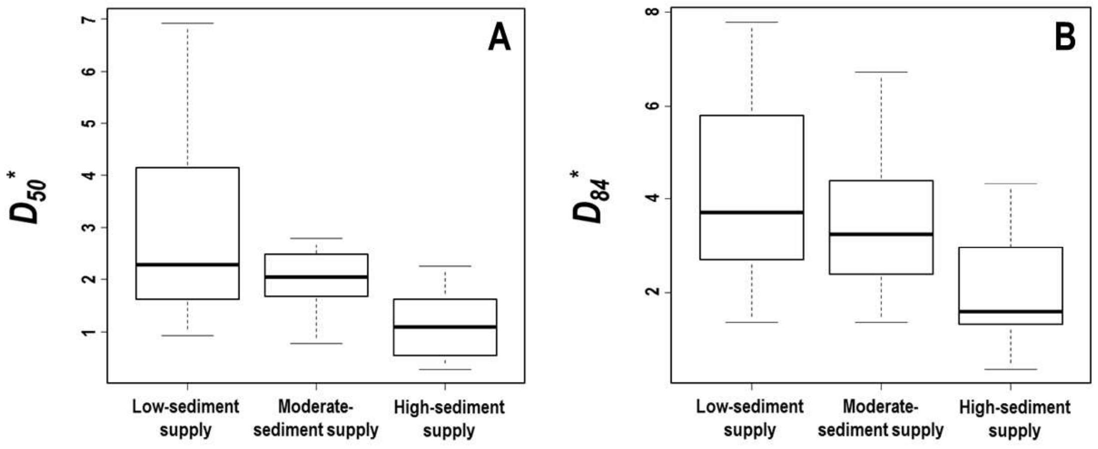

Figure 5. Differences in armour ratios according to sediment-supply conditions at the catchment scale. See main text. A: D_{50}^*. B: D_{84}^*.

However, the compiled data illustrate how a certain degree of surface armouring ('armour ratios' >1) can also be observed in rivers fed by significant sediment supplies (Figure 5). Therefore, non-degrading gravel-bed streams with considerable sediment inputs may also exhibit some armouring. In truth, bedload transport models (Wilcock and DeTemple, 2005), tracer studies (Haschenburger and Wilcock, 2003), flume experiments (Hassan et al., 2006), and field observations (Andrews and Erdman, 1986; Clayton and Pitlick, 2008; Haschenburger, 2017) support the occurrence of such 'mobile' armours and suggest their persistence even during large floods. The sheltering of small particles into pockets and interstices between coarse grains can contribute to the development of these coarsened surfaces in well-supplied rivers (Parker et al., 1982; Parker and Klingeman, 1982; Andrews and Erman, 1986; Andrews and Parker, 1987; Berni et al., 2018). Surface coarsening represents in these cases an effective mechanism allowing for the transport of the coarse fractions in the gravel load at the same rate as those which are finer (Parker and Klingemann, 1982; Parker and Toro-Escobar, 2002; Parker, 2004). As such, it leads to a progressive equalization between the bedload and the subarmour GSDs (Parker and Klingemann, 1982; Marion and Fraccarollo, 1997; Mario et al., 2003; Mao et al., 2011; Powell et al., 2016; Bertin and Freidrich, 2018), a situation referred to as 'dynamic' or 'mobile armours'. Moreover, in gravel-bed rivers, the amount of entrained bed material and the grain size of the bedload increase as flow discharge rises (Milhous, 1973; Jones and Seitz, 1980; Kuhnle and

Willis, 1992; Andrews, 1994; Wathen et al., 1995; Powell et al., 2001; Ryan and Emmett, 2002; Wilcock and McArdell, 1993, 1997; Clayton and Pitlick, 2008; Pitlick et al., 2008; Recking, 2016). We could, thereby, expect differences in mobility between different grain-size classes with fluctuations in flow discharge. Therefore, selective transport and horizontal winnowing of fines during recession limbs and/or low flows may exhaust the fine sediment and favour the development of a cover of coarse material preventing further sediment transport (Harrison, 1950; Gessler, 1970; Little and Mayer, 1972; Proffitt and Sutherland, 1983; Chin et al., 1994). In this regard, perennial and seasonal streams subjected to long-lasting floods and sustained receding limbs might have more chances of suffering a coarsening of their bed surfaces and thus become more armoured. In the opposite extreme, we could consider streams experiencing flashing-flood hydrology. A flash flood involves a sudden increase of peak flows, bed shear stresses and equal mobility for all the particle sizes represented in the streambed (Laronne and Reid, 1993; Laronne et al. 1994; Reid and Laronne, 1995). In such cases, we should not expect large differences between the surface, subsurface and bedload GSDs (Dietrich et al., 1989; Chin et al., 1994; Powell et al., 2001; Parker, 2008; Venditti et al., 2017; Bertin and Friedrich, 2018). As a result, streams receiving comparable amounts of sediment inputs may exhibit different armour ratios depending on the dominant hydrological regime (Hassan et al., 2006).

Unfortunately, the compiled data are mostly from mountain streams dominated by snowmelt flow regimes, probably because planning field-campaigns in order to measure bedload is easier in this kind of rivers compared to rainfall-dominated settings, where it is more difficult to know in advance when a channel-forming flow is going to occur (also to monitor within a fairly deep flow channel with long rising and falling limbs). Thus, it is not easy to explore in depth the influence of hydrological regime with the available data. In any case, snowmelt-dominated rivers, usually submitted to sustained floods during the melting season, tend to show larger armour ratios than rainfall or flash-flood dominated streams (see dotplot shown in Figure 6). Furthermore, the percentage of fine sediment also tends to be lower in these snowmelt-dominated streams (Figure 6B), indicating fine sediment depletion during the long and gradually declining limbs of typical snowmelt hydrographs. On the other hand, glacial-fed rivers, which normally have high-sediment

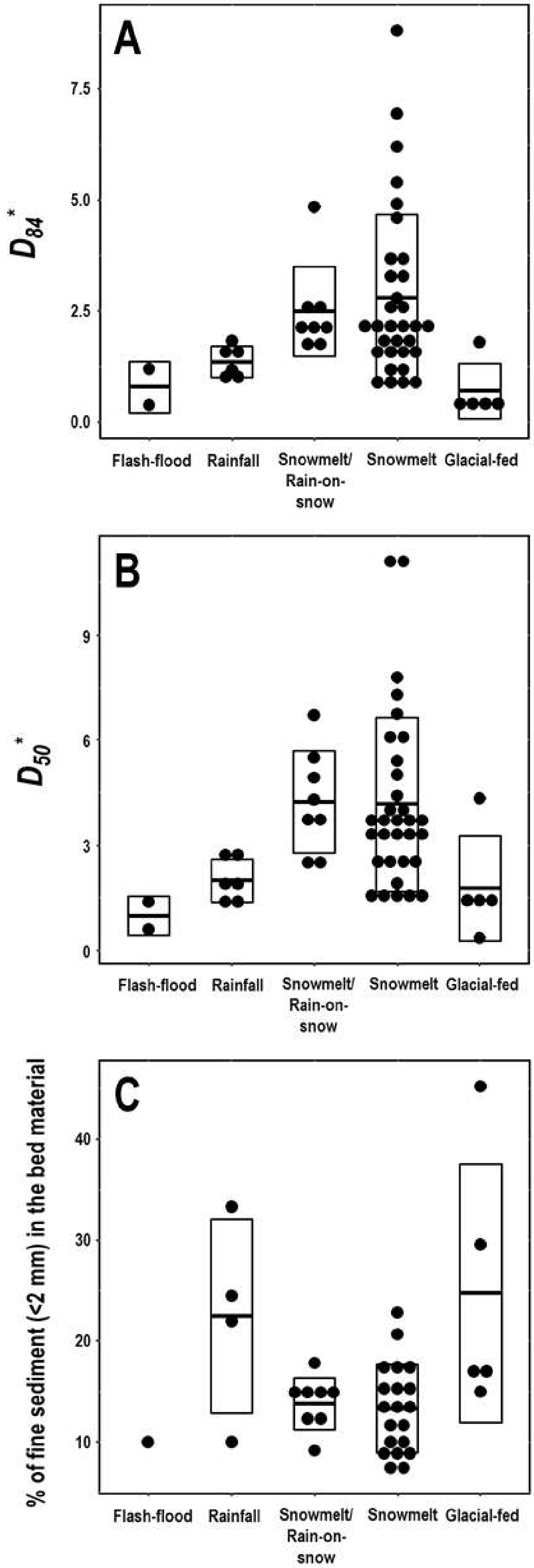

Figure 6. Differences in armour ratios (A and B) and percentages of fine sediment (C) according to the dominant flow regime.

supplies from glacial/periglacial sources (particularly the 'glacial flour' transported from glaciated upland basins), show relatively low armour ratios (Figure 6B). The influx of fine sediments represented by the glacial flour may help the coarse grains composing the armour layer to become more mobile (Cui et al., 2003; Venditti et al. 2010a, b; Yager et al., 2015). In addition, the flow regime of glacial-fed rivers is often characterised by daily peaks of discharge, rising and falling successively, and these somewhat shorter, rapidly changing hydrographs are less prone to promote armouring (Hassan et al., 2006). Hence, in conjunction, both issues may determine the relatively low armour ratios documented here in the case of glacial-fed rivers.

To summarize, our review of field data shows how sediment supply, together with the shape of the dominant flood hydrographs, condition surface armouring in gravel-bed rivers. The hydrological regime controls the rate at which bedload and fine sediment are winnowed and exhausted during the course of transport events. For instance, we can expect a less armoured surface if a continuous replenishment of sediment exists during the transport episode, as we can reasonably expect for glacial fed streams. In the opposite extreme, we can anticipate a better developed armouring and a streambed surface more depleted in fines in cases where the bedload is exhausted, which is likely when streams are subjected to long-lasting snowmelt hydrographs. This is in accordance with the set of flume experiments by Hassan et al. (2006) who investigated the influence of different hydrographs on surface armouring and observed varying textural responses to steady vs. gradually varying flows. Nevertheless, fine sediment depletion during floods may take more or less time depending on the amount of sediment supplied from upstream sources. Therefore, the rate at which bedload is supplied into the channel may modulate the effects of flow hydrographs and strongly determine the rate and degree of fine sediment depletion, and consequently the degree of armour development.

3.3. Surface armouring and streambed mobility

As stated above, surface coarsening is associated with fine sediment exhaustion from the streambed and the development of clast arrangements and imbrications (Church et al., 1998; Venditti et al., 2017). The increase of particle stability linked to surface structuration may involve a decrease in the frequency of clast mobility and streambed disorganization (Church et al., 1998;

Hassan and Church, 2002). To further explore this issue, we introduce a new metric: the 'transport stage' ratio (τ^*/τ_c^*). This is defined as the ratio between the peak basal shear stress for a given flow discharge and its critical value for incipient sediment motion. Critical stresses for sediment entrainment were estimated here based on Recking's (2013) fit for D_{84} (see supplementary files for more information about how we computed transport stage ratios).

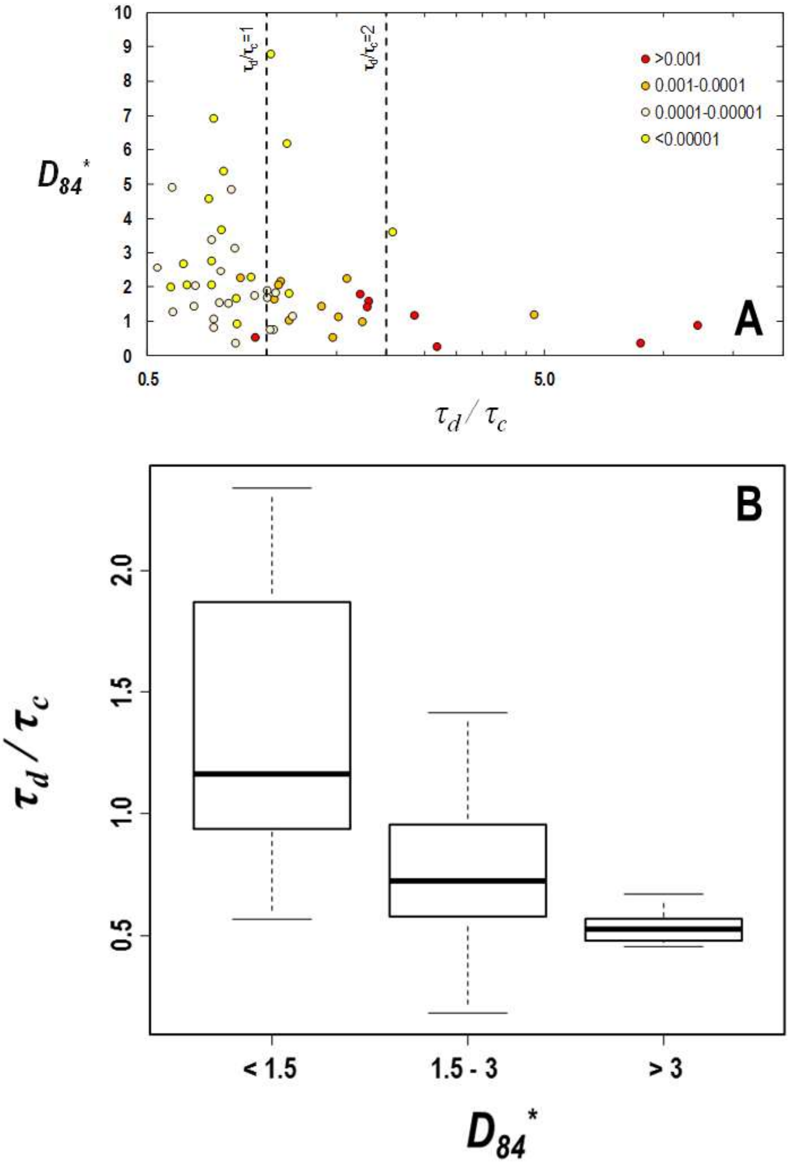

Figure 7. A: Armour ratio (D_{84}^*) plotted versus the transport stage (τ_d/ τ_c). B: Transport stages values at the dominant discharge in poorly armoured ($D_{84}^* < 1.5$), normally armoured ($1.5< D_{84}^* < 3$) and well armoured ($D_{84}^*>3$) rivers. Critical threshold Shields values (τ_c) were computed using Recking, 2009).

Values of this metric, estimated at the dominant channel-forming discharge, are close to the critical thresholds for entrainment of the coarser fraction of bed sediment in well-armoured streams (Figure 7A). However, in poorly armoured streams, Shields stresses are well above these critical values. These poorly armoured streams also show larger bedload fluxes (see the values for transport intensities in Fig. 7A). A turning point can be defined close to an armour ratio of ~2:

there are no channels with large transport intensities (ϕ > 0.0001) and high transport stages at dominant discharge (τ^*/τ_c^* > 2) for armour ratios larger than 2. These observations confirm that overall streambed mobility would be larger in poorly armoured streams, and document how well-armoured streambed surfaces are seldom moved. Considering all of the above, the compiled data support the idea of surface armouring being conditioned by dominant sediment supply conditions (section 2.2), with 'static-armours' characterised by larger armour ratios than 'mobile-armours' (Figure 7B).

3.4. Quantifying sediment supply conditions in gravel-bed rivers

Our review of the literature clearly shows how the GSD of a streambed's surface, at a given river reach, adjusts to the volume of sediment inputs and the ability of the channel to export the available sediment inputs (Figures 6 and 7), an idea already outlined by previous field and flume studies (Dietrich et al., 1989; Venditti et al., 2017). Introducing metrics allowing the quantitative description of the sediment supply is then of interest as shown by Dietrich et al. (1989) who proposed their own metric (q^*) (Dietrich et al., 1989; Montgomery and Buffington, 1997; Venditti et al., 2017):

$$q^* = \frac{q_{s_s}}{q_{s_{ss}}} \qquad \text{Eq. 2}$$

where q_s refers to the bedload transport rate per unit width and the subscripts *s* and *ss* to the surface and subsurface sediment, respectively. The 'bedload supply' index as defined in eq. 2 is the ratio between the sediment transport capacity to mobilize the surface GSD and the capacity to recruit sediment from a hypothetical surface as fine as the subsurface. When actual bedload rates match the bedload transport capacity of the channel, q^* should equal 1. Conversely, if sediment inputs into the channel are lower than transport capacities, then $q^* < 1$. Here we computed the q^* ratio, based on flow characteristics at the representative channel-forming discharge and on Recking's equation (details on q^* calculation are explained in the supplementary information, Subsection S.3). The obtained values of q^* are in good agreement with our initial classification of compiled data as high-, moderate- and low-sediment supplied channels (Figure 8A).

However, the ‘bedload supply’ index q^* has the problem of estimating bedload transport capacity of a channel for a hypothetical situation where the streambed’s surface GSD equals its subsurface GSD (q_{ss}, denominator in eq. 2). In the field cases compiled here, this required the application of a bedload equation for the estimation of q_{ss}, with all the uncertainties linked to choosing the right formula. For that reason, we propose a simpler metric to quantify the ratio between the flux of sediment entering a given river reach, and the capacity of the channel to transport that sediment downstream: the ratio between bedload fluxes (q_s) and stream power (ω) at the representative or dominant channel-forming discharge. This metric quantifies the mass of sediment carried by a river with a given amount of hydraulic power. Values of this ratio are in good agreement with our initial classification of the compiled data as high-, moderate- and low-sediment supply channels (Figure 8B), confirming its usefulness for characterizing the dominant sediment supply conditions in gravel-bed rivers.

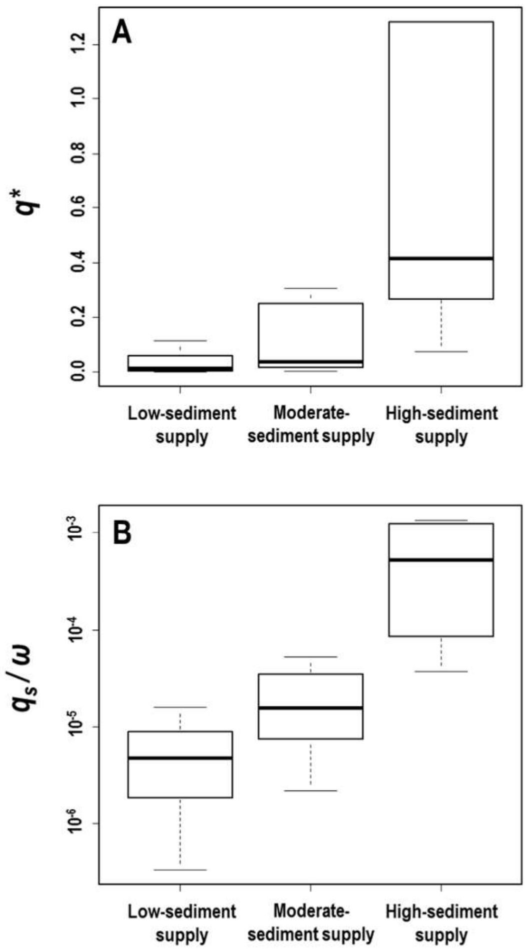

Figure 8. Differences in sediment-supply metrics (q^* and q_s/ω_d) according to our initial classification of data as low-, moderate- or high-sediment supply streams (see the main text). A: sediment supply metrics proposed by Dietrich et al. (1989). B: our own sediment supply metrics (see main text).

4. Meta-analysis on the data: linking streambed texture, sediment supply and hydrological regime

4.1. Surface armouring driven by sediment supply

Based on their own flume experiments, Dietrich et al. (1989) already observed that D^* increases while sediment feed decreases compared to the overall bedload transport capacity of the channel. Using Meyer-Peter and Muller's (1948) bedload transport equation, these authors described the links between surface armouring (D_{50s}/D_{50ss}) and sediment supply (q^*) as:

$$q^* = \left(\frac{\frac{\tau}{\tau_{c_{ss}}} - D_{50}^*}{\tau/\tau_{c_{ss}} - 1}\right)^{1.5} \qquad \text{Eq. 3}$$

where τ is the basal shear stress and τ_{css} is the critical shear stress for the inception of motion in the subsurface sediment. At the time when Dietrich et al. (1989) published their work, using Meyer-Peter and Muller's (1948) bedload equation made sense due to its simplicity and its common use in sediment transport studies. However, more sophisticated bedload transport formulas have been proposed since then (e.g. Wilcock and Crowe, 2003; Recking, 2013), which proved to perform well for 1D computations of bedload in natural gravel-bed streams (e g. Parker, 2004; Recking, 2010; Camenen et al., 2011; Vázquez-Tarrío and Menéndez-Duarte, 2015; Hinton et al., 2018). In this paper, based on Recking's (2013) (after Recking et al., 2016) bedload equation, the following expressions are obtained (see details in the supplementary information):

$$D_{84}^* = \frac{1}{f} \cdot {q^*}^{-1/5} \qquad \text{for partial-mobility conditions} \qquad \text{Eq. 4}$$

$$D_{84}^* = {q^*}^{-1} \qquad \text{for full-mobility conditions} \qquad \text{Eq. 5}$$

where f in eq. 4 is a parameter relating D_{50}^* to D_{84}^* (~1.4, according to Figure 2). Eqs. 4 and 5 provide a simple mathematical description of how D^* should correlate and change with q^*. As opposed to eq. 3, eqs. 4 and 5 use D_{84}^* rather than D_{50}^*, because Recking's (2013) equation works with the 84-th percentile of the surface GSD as the reference bed sediment size.

In Figure 9 we have plotted D_{84}^* against q^* for the field data, the latter estimated from flow characteristics at the dominant channel-forming discharge and Recking's equation (details on q^* calculation are explained in the supplementary information). We have also incorporated into this plot data from flume experiments (extracted from Venditti et al., 2017; see supplementary information), which tend to overlap the field data: armour ratios change with bedload supply following a similar trend in flume and field data. Additionally, the obtained fit is very close to the curve defined by eq. 4 (low-transport stage conditions). This suggests that partial mobility conditions may dominate bedload motion at the dominant discharge in well-armoured streams.

We also plotted armour ratios against q_s/ω ratios (Figure 10A), and the data show a moderate but statistically significant correlation between the q_s/ω ratio and the armour ratios. As shown above (Figure 4), D_s is partially controlled by D_{ss}. This covariation may be introducing some noise in the plot shown in Figure 10A. In order to remove this effect, we propose a new version of the armour ratio (D^{**}):

$$D^{**} = \frac{D_S}{D_{SS}^{\beta}} \qquad \text{Eq. 6}$$

where β is the parameter defining how surface grain-size scales to subsurface grain-size. According to Figure 4, β is ~ 0.62 and ~0.41 for D_{84} and D_{50}, respectively. This 'corrected' version of the armour ratio shows a stronger correlation to the q_s/ω ratio (Figure 10B). Similar to Figure 9, Figure 10 shows how streambed surface tends to coarsen with decreasing sediment supplies (proxied here by the q_s/ω ratios).

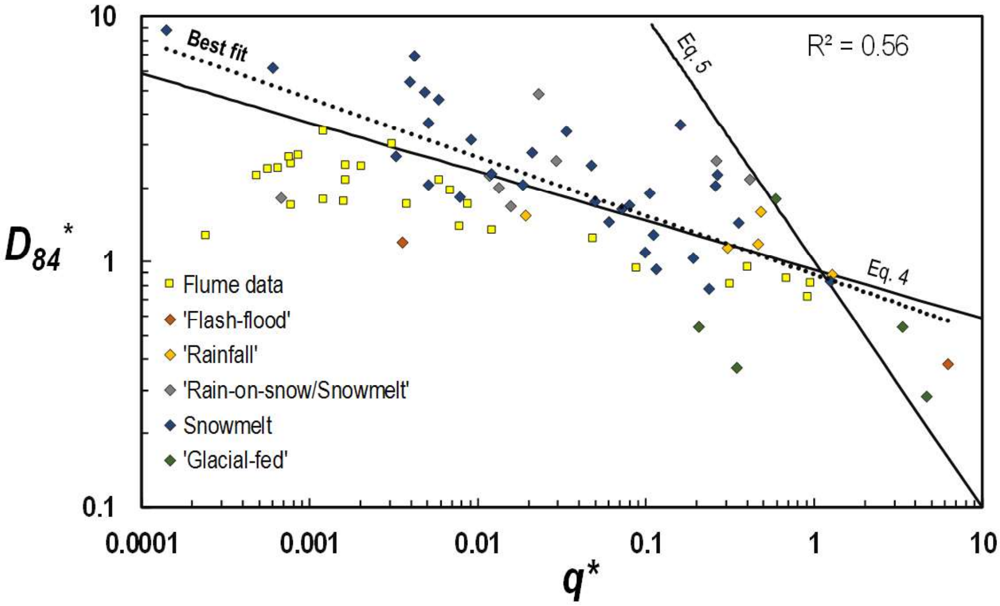

Figure 9. Armour ratio plotted against the 'bedload supply ratio' q^* (see main text for more details).

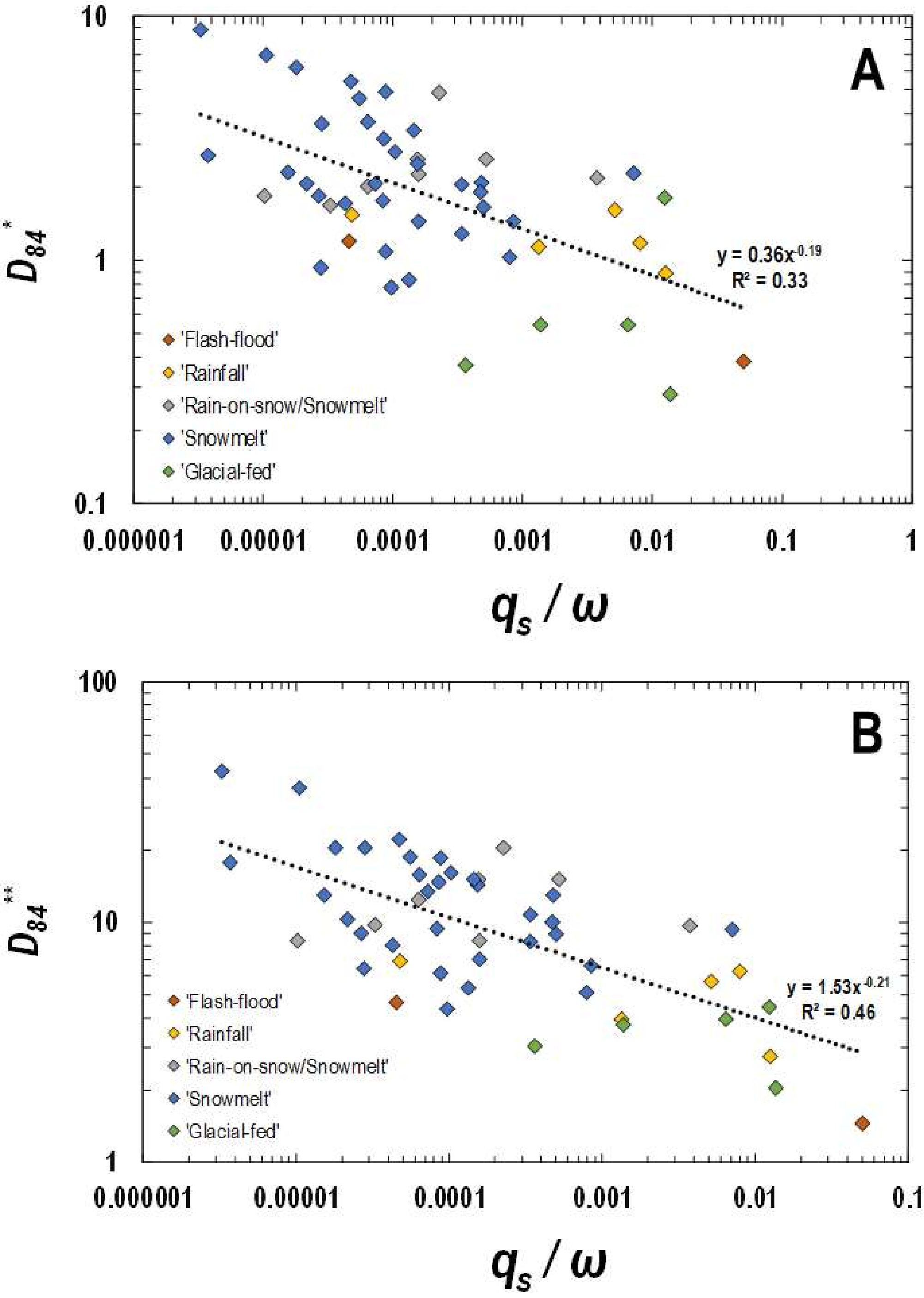

Figure 10. Armour ratio (A) and corrected armour ratio (B) plotted versus the ratio between bedload fluxes and streampower (q_s/ω_d).

Although the number of plots is not well balanced across the different groups of data, it is worth pointing out that in Figures 9 and 10 rainfall data tend to plot close to the regression line, while snowmelt data tend to show a larger scatter and broader range of armour ratios. Snowmelt systems are typically located in the upper parts of the catchment compared to rainfall streams, which are usually located downstream, further from the coarser sediment sources. Consequently, this implies that rainfall streams will be somewhat less prone to develop larger armour ratios even if their sediment supply is limited. In this regard, large armour ratios may have some dependence on the upstream/downstream location of the stream and its particular geological context, as already suggested by Pitlick et al. (2008).

4.2. Hydrological controls on surface armouring

Figures 9 and 10 clearly show how streambed surface evolves and becomes progressively armoured with declining sediment supplies. Nevertheless, there is a certain amount of scatter in both plots, which highlights that some variability in armour ratios may exist with a given sediment supply. Indeed, data from snowmelt streams tend to plot in the upper envelope of the point cloud in Figure 9 and, conversely, data from glacial-fed and flash-flood dominated streams tend to fall in the lower envelope, while flume data project in the middle of the point cloud, together with rainfall dominated rivers. Similarly, in Figure 6 snowmelt dominated streams tend to show larger armour ratios and smaller q_s/ω ratios than rainfall, flash flood and glacial-fed dominated streams. All these observations highlight the variability in surface armouring and sediment supply conditions and their interplay with different hydrological regimes.

However, we should also consider that adjustments of the streambed to shifts in sediment supply conditions are not always synchronous and there is potentially a lag between the two. For instance, surface coarsening slowly propagates downstream after widespread land cover changes in the upland basin or downstream from a dam (Rollet et al., 2013), so it can take several years before we observe riverbed coarsening following a significant upstream perturbation. Furthermore, in snowmelt systems, some hysteresis in bedload supplies can be observed over the hydrological year (Moog and Whiting, 1998); for instance, there can be significant bedload transport for a given discharge in early spring, while bedload rates are reduced for similar flow discharges occurring at the end of the flood season (Misset et al., in press). We have not controlled for all these variables, so they probably introduce additional scatter in the relations between surface armouring and sediment supply reported here.

4.3. Quantifying the variability in armour ratios

Based on the analysis performed in Subsections 4.1 and 4.2, we can conclude that surface coarsening accommodates to the dominant sediment supply conditions, but the rate at which bedload is emptied during the course of transport episodes may modulate the streambed adjustment to sediment supply. This may complicate the use of armour ratio for river diagnosis, insofar as the dominant sediment supply conditions are not the only drivers of surface grain-size in gravel-bed rivers. The rate at which fine bedload exhausts during floods, the seasonal variability in sediment availability and the time lag before the riverbed starts to respond after a significant shift in the upstream bed material supplies also have a non-negligible impact on the armour ratios documented at a given river reach. All these constraints may be largely dependent on site-specific controls, such as the cross-sectional extent of armour break-up, the shape and duration of the flow hydrograph, and the local availability of loose and fine sediment coming from upstream reaches and bank toes.

In this regard, Figures 9 and 10 not only illustrate how surface coarsening scales with sediment supply, but also show the range of potential variability in armour ratios for a given sediment supply and observed within the compiled field data. That said, we could report rivers more or less armoured than the streambed conditions expected for an 'average behaviour' with a given bedload input, reminiscent of the old distinction between 'static' versus 'mobile' armours (Jain, 1990; Parker and Sutherland, 1990), so we refer to more (or less) mobile armour layers than the average mobility expected for a given sediment supply condition (defined by the best fit in Figures 9 and 10). To handle this variability, we performed a quantile regression analysis and plotted the regression between the different percentiles of the D^* distribution and the sediment supply metrics (q^* and q_s/ω), obtaining two diagrams that illustrate the likelihood of a given value of D^* (Figure 11A) or D^{**} (Figure 11B) with a given sediment supply. Fluctuations from the 1-st to the 99-th percentiles are linked to a set of factors, which include differences in the hydrological regime, seasonal variability and time passed after significant shifts in upstream sediment inputs. Thus, Figures 11A and 11B can be easily combined with some available qualitative information on a

406 specific study site in order to have an idea of the most probable values for the armour ratio with a given sediment supply and hydrological regime.

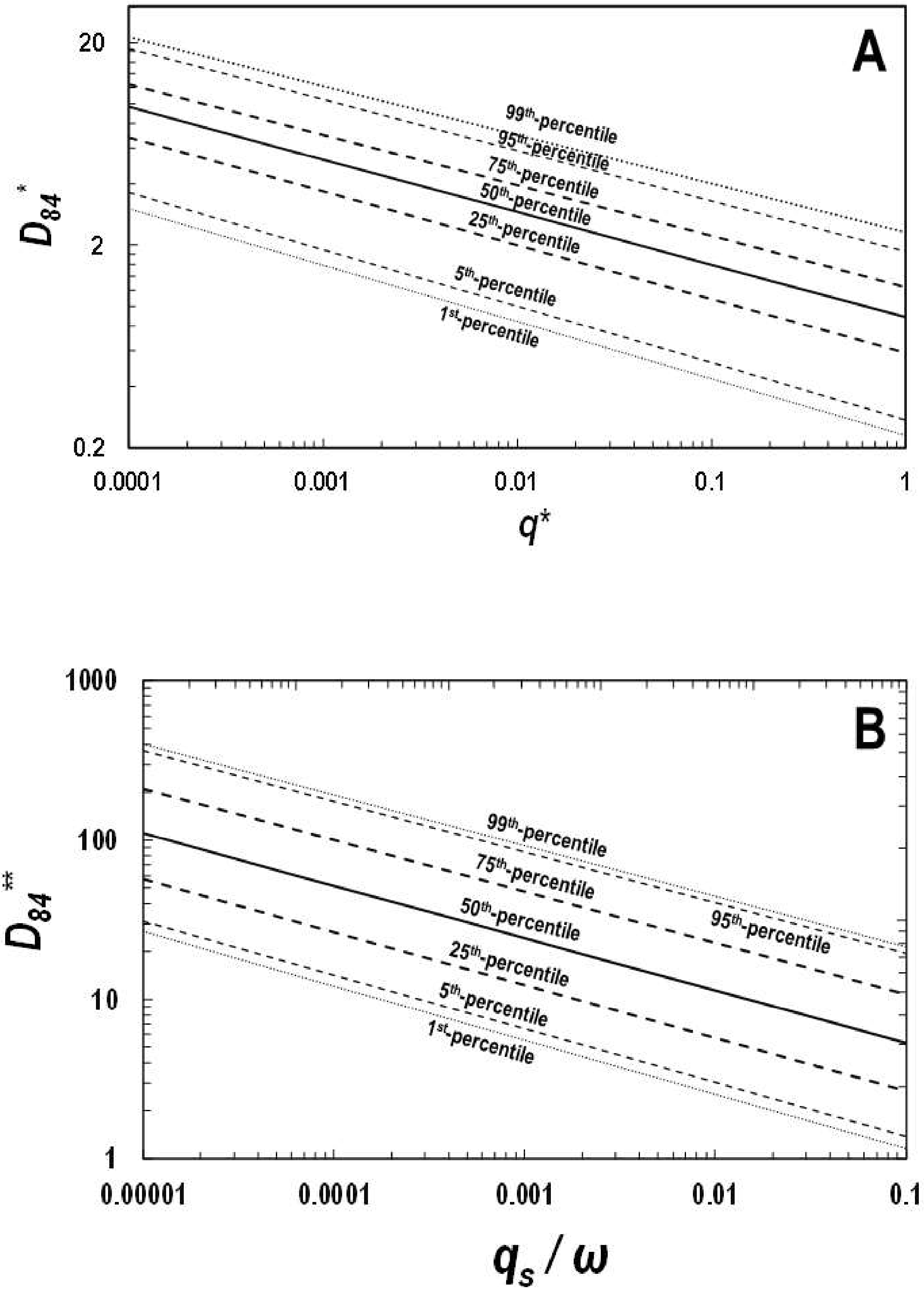

Figure 11. Diagrams issued from quantile regression analysis of the compile data, defining the likelihood of a certain value of the armour ratio according to sediment supply metrics (see main text for more details).

4.4. Studying links between bedload transport, channel morphology and surface armouring

Streambed surfaces adjust to available bedload yields (Figures 9 and 10). Reciprocally, surface coarsening controls the frequency and magnitude of armour breakup and streambed disorganization during floods (Figure 7). Strongly armoured streambeds are more difficult to disorganize and more infrequently moved. Therefore, we could expect a lower degree of bed material recruitment into bedload during regular flows. With this in mind, we expected surface armouring to have some control over bedload rates. In order to explore this issue, we took the available information on bedload discharges (Table 1) and performed a multiple regression analysis linking bedload rates to flow magnitude and armour ratios:

$$\phi = \left({}^{Q}/_{Q_d}\right)^{a} \cdot (D_{84}^{*})^{b} \qquad \text{Eq. 7}$$

where ϕ is bedload transport intensity (see supplementary information), and Q/Q_d is the ratio between the peak discharge for the transport episode and the dominant discharge (hereinafter called flow ratio). However, the wide diversity of channel morphologies represented amongst the compiled data should be highlighted, since channel macroforms control flow and sediment transport patterns, which in turn may potentially affect bedload rates (Ferguson, 2003; Francalanci et al., 2012; Recking et al., 2016; Vázquez-Tarrío et al., 2018; Vázquez-Tarrío and Batalla, 2019). For this reason, we introduced a set of three binary indicators into the regression analysis to incorporate into it the influence of channel morphology:

$$\phi = \left({}^{Q}/_{Q_d}\right)^{a} \cdot (D_{84}^{*})^{b} \cdot e^{c \cdot RP} \cdot e^{d \cdot SP} \cdot e^{d \cdot BR} \qquad \text{Eq. 8}$$

where RP, SP and BR are the dummy variables taking a value of 1 in the cases of riffle and pool, step-pool and braided channels, respectively. In the case of plane-bed channels, the three dummy variables would be 0.

To test whether eqs. 7 and 8 fit the available bedload information, we used ordinary multiple regression in linearized form and stepwise procedures, after log transforming all the variables included in the equation. Both equations explain the variance in the compiled bedload data to a statistically significant degree, with all the variables included in the regression model being significant (Table 5). The R^2 values imply that eq. 8 is more robust than eq. 7 (R^2 = 0.60 vs. 0.34, respectively), which outlines the existence of some morphological imprint on bedload transport rates. According to the regression model, transport intensities increase with the 1.7 positive power of flow ratios. Conversely, bedload rates are negatively correlated to armour ratios, i.e. bedload rates tend to be considerably weaker in well-armoured channels. With the aim of assessing the relative importance of each of the independent variables incorporated into the regression model, we used the method proposed by Lindeman et al. (1980), often recommended for assigning shares of relative weight of predictors to the R^2. According to this analysis, channel morphology is the variable that explains the largest amount of variability in bedload data (~53 % of R^2), followed by flow magnitude (23% of R^2) and armour ratios (21% of R^2). Differences in dominant channel morphology have a strong effect on the variability in bedload rates observed between the compiled data, but differences in surface armouring also have a large impact.

Variable	Coefficient	Standard Error	t	*p-value*	VIF[1]
Intercept	2.991×10^{-5}	0.077	-135.680	0.000	
Q/Q_d	1.671	0.035	45.156	0.000	1.099
D_{84}^*	-2.371	0.063	-37.520	0.000	1.565
BR	0.809	0.264	3.067	0.002	1.257
RP	4.482	0.077	57.921	0.000	1.155
SP	1.557	0.125	12.453	0.000	1.273

Residual standard error: 2.579 on 5470 degrees of freedom
Multiple R^2 = 0.60; Adjusted R^2 = 0.60
F-statistic: 1611 on 5 and 5470 degrees of freedom. *p-value* = 2.2×10^{-16}

[1] Variance Inflation Factor

Table 5. Results from the multiple regression model based on eq. 8 (see main text).

Different channel morphologies and macro-bedforms result from the adjustment of channel macro-roughness to different balances between sediment supply and transport capacity (Montgomery and Buffington, 1997); similarly, armouring is the consequence of the adjustments in roughness at the grain-scale to the same balances between sediment supply and capacity (Dietrich et al., 1989; Venditti et al., 2017). Consequently, both dominant channel morphology and armour ratios constitute a proxy of sediment supply and should be related. Interestingly enough, we have observed systematic differences in armour ratios between the different channel morphologies (see Figure 3). In general, multi-thread channels and rivers with riffles and pools exhibit a lower degree of surface armouring, while plane-bed and step-pool channels show higher armour ratios. Higher armour ratios in step-pool channels could be related to the existence of jammed stones and large immobile boulders that may contribute to larger armour ratios. In plane bed channels, large protruding grains and immobile stones defining transversal ribs and cells are also common (Church et al., 1998), and may help define a surface coarser than in riffle and pool and braided channels. Following this, eq. 8 would provide a mathematical expression describing how the increase in bedload rates with flow discharge is modulated by the differences in sediment supply, which is parameterised through the armour ratio and the dummy variables (i.e. dominant macro-bedforms). In Figure 12, we compare the transport intensities estimated using eq. 8 to the true values measured in the field. Regression predictions plot close to the 1:1 line, with an average 0.9 ratio between predictions and truth-values and 43% of points showing a discrepancy lower than one order of magnitude. Riffle and pool and braided data show a larger scatter than plane-bed and step-pool morphologies; this is probably related to the larger cross-sectional variability in shear stress and sediment paths, typical of these channel settings (Recking et al., 2016; Vázquez-Tarrío et al., 2018).

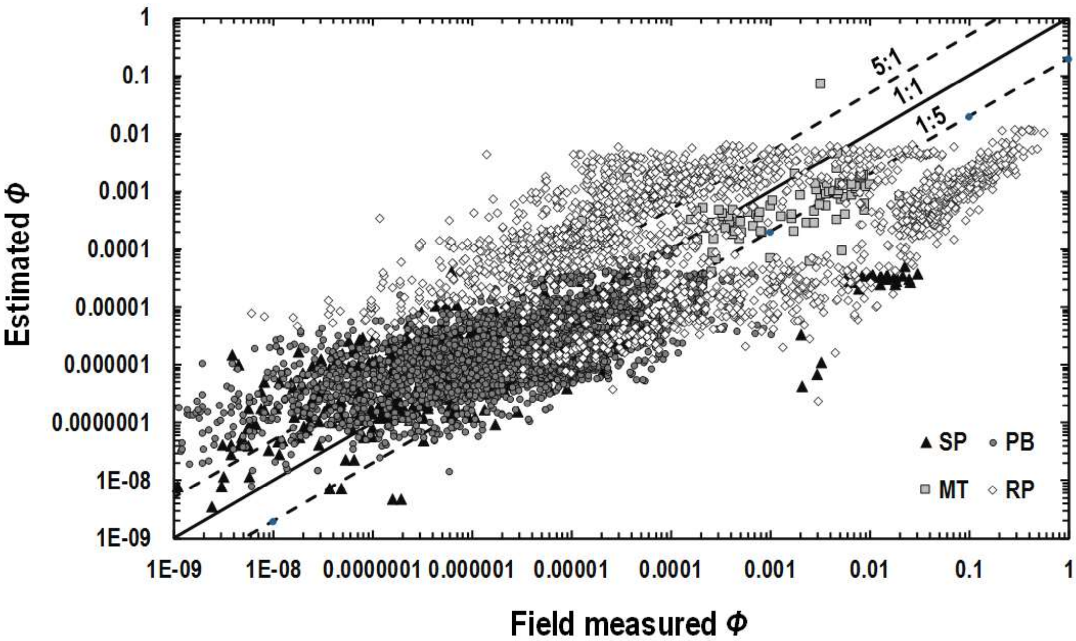

Figure 12. Bedload transport intensities estimated using eq. 8 plotted versus transport intensities measured in the field. MT: Multi-thread channels; PB: Plane-bed; RP: Riffle and pool; SP: step-pool streams.

5. Discussion

5.1. Sediment supply accommodated through armouring in gravel-bed rivers

Our meta-analysis shows a decline in the armour ratio with increasing bedload supplies (quantified through the q^*-metrics and q_s/ω_{dd}) in the compiled field data (Figures 7 and 8), which is similar to the trends observed in previous flume experiments (Dietrich et al., 1989; Venditti et al., 2017). In this regard, plots shown in Figures 7 and 8 quantify the important imprint of sediment supply over surface armouring in gravel-bed rivers. It should be noted that q^* was computed based on subsurface GSD, using the common approach of equalling subsurface GSD to the average GSD of the bedload. However, bedload capacities would be more adequately computed based on the actual GSD of the bedload. There may be situations where shifts in sediment sources and catchment patterns of sediment production could lead to changes in the grain size of the sediment supplies; for instance, mountain watersheds submitted to massive afforestation (or forest clearance), or river reaches fed by largely managed (e.g. dammed, dredged) tributaries. In such situations, we would expect changes in the GSD of the bedload (fining or coarsening) that may derive in a change in bedload transport capacities; this would in turn influence surface GSD together with changes in the amount of sediment inputs.

There is a certain amount of unexplained scatter within the data in Figures 7 and 8, so there should be other contributing and explanatory variables for data variance in them apart from bedload supply. We believe that the variability introduced by differences in the shape of the dominant competent flow hydrograph and flow duration (Hassan et al., 2006; Phillips et al., 2018) are the most probable candidates. These flow parameters would be largely variable amongst the selected study reaches and could not be described by a single q^* or q_s/ω ratio based only on peak discharge. As pointed out above, gravel-bed streams submitted to long receding hydrograph limbs and experiencing several floods per year are likely to develop a higher degree of armouring than equivalent streams in terms of sediment supply, but experiencing less frequent flooding and a short falling limb (Hassan et al., 2006). Therefore, flood hydrograph may exert an important control on armouring, together with sediment supply. Although the available data do not let us explore this issue in much depth, in general they are in agreement with this general picture:

snowmelt-dominated data tend to show larger armour than rainfall-dominated rivers in Figure 6, although the possibility of time lags between previous changes in upstream sediment inputs and streambed adjustment, or even some seasonal variability in sediment supply, should not be dismissed, since both may play a role in the variability documented in the compiled data. The influence on armouring of these time lags and seasonal variability in sediment inputs may be more important in those channel morphologies better coupled or connected with upstream sediment sources (e.g. braided channels), where one-shot observations of armour ratios may not detect well the average trends.

However, despite the scatter in the data, the overall picture shown by Figures 9 and 10 illustrates how the signal linked to differences in sediment yields is the dominant one, and it is globally well-recorded through the surface grain size and the armour ratio in gravel-bed rivers. Our analysis suggests that sediment supply drives streambed surface GSD in gravel-bed rivers in two different ways: i. the GSD of the sediment supplied and introduced into the channel network exerts an obvious control, since it defines the range of grain sizes that are available in the bed material (Figure 4); ii. streambed surface represents the sediment layer in more intimate contact with fluid forces, so it adjusts to the balances between volumes of sediment supplied into the channel and the streams' capacity to transfer these sediment inputs downstream out from the reach (Figures 9 and 10). In principle, stream ability to convey sediment inputs downstream is size-selective (Paola and Seal, 1995), and this partially explains why the surface layer tends to coarsen. This influence of hydraulic conditions could be eventually more important and partially blur the primary influence of the GSD of the bedload.

Based on our data and quantile regression analysis, we have created two diagrams illustrating the likelihood of a certain armour ratio for a given sediment supply (Figure 11). We believe these diagrams provide a useful frame to interpret armour ratios measured in the field, and to characterize streambed state and mobility in a quick way. For many applied issues (channel-design, river restoration), an adequate diagnosis of the hydro-morphological status of a given reach is fundamental. However, information of bedload fluxes is lacking in many cases. In such cases, armour ratios measured in the field may provide a quick characterization of the sediment supply conditions and streambed mobility of the considered river reach, by combining diagrams such as those shown in Figure 9 with some qualitative knowledge about the dominant hydrological regime.

5.2. Implications for equilibrium channel geometry

We observed how in most of the compiled data shear stresses at the dominant discharge are close to critical thresholds for sediment motion (Figure 10). These observations reflect the streambed's surface adjustment to dominant hydraulic conditions. In this respect, theoretical work (Parker, 1978; Parker, 1979) and decades of observations in gravel-bed alluvial channels (Parker, 2004; Mueller and Pitlick, 2005; Parker et al., 2007) supported the hypothesis of threshold or near-threshold channels (Parker et al., 2007; Phillips and Jerolmack, 2016; Métivier et al., 2017). According to this idea, alluvial channel dimensions adjust in such a way that the threshold for the motion of median-size grains occurs close to bankfull flows (e.g. MacKenzie et al., 2018). However, in our data Shields values at the dominant discharge are close to the critical thresholds for the entrainment of the coarser fraction of bed sediment only in well-armoured streams (Figure 10); otherwise, Shields stresses are well above these critical values in poorly armoured streams. Pfeiffer et al. (2017) observed that only supply-limited streams meet the threshold channel condition, while in capacity-limited systems they reported Shields stresses at bankfull considerably over the critical levels. Based on these observations, these authors concluded that the common observation of channels adjusting to threshold conditions simply reflects the fact that the channels most commonly surveyed in the field are subject to modest sediment supplies. Nevertheless, we propose an alternative interpretation for the trends shown in Figure 10 and Pfeiffer et al. (2017). According to the data analysed in this manuscript, high-sediment supply systems correspond mainly to multi-thread and riffle-pool streams (Figure 3). These kinds of settings are characterized by bar morphologies, which involve complex 3D flow structures (Francalanci et al., 2012), specific patterns of grain size sorting (Paola, 1989; Lisle et al., 1992) and a great variability in shear stress distributions across their cross-section (Recking, 2009; Recking et al., 2016). Furthermore, gravel dunes and bedload sheet propagation (Venditti et al., 2017) represent an additional source of form roughness in these rivers. Consequently, we expect larger biases in bedload estimates when averaging shear stresses across the cross section of these streams (Recking, 2013). Therefore, it is possible that 1D averaged shear stresses are not an adequate proxy for the actual variability in shear stresses acting at the local and grain scales in riffle and pool and multi-thread settings. This may explain the observed deviation from near-threshold conditions, which could be to a large degree an artefact resulting from the assumptions made when estimating cross-section averaged shear stresses (Yager et al., 2018).

5.3. Armour ratio: a proxy for the channel planform configuration

Our review outlined differences in armour ratios according to channel morphology (Figure 3), with multi-thread and riffle and pool rivers exhibiting, in general, a lower degree of surface armouring than plane-bed and step-pool channels. The scale of the roughness and protruding elements in step-pool channels is in general larger, with channel-spanning ribs (steps) composed by an accumulation of jammed cobbles and boulders transverse or oblique to the channel (Zimmermann and Church, 2001; Chin and Wohl, 2005), alternating with pools (Church and Zimmermann, 2007; Lamarre and Roy, 2008). Step-pool streams are normally close to headwater areas and are largely dependent on the accumulation of relatively fine colluvium inputs into pools and around protruding boulders (Turowski et al., 2011; Recking, 2012; Recking et al., 2012; Piton and Recking, 2017). Accordingly, protruding cobbles and boulders can be found on the bed surface of step-pool channels, even with large sediment supplies and thick alluvial covers. This may explain the generally larger armour ratios observed for step-pool streams. Similarly, the data for braided rivers tend to show lower armour ratios (Figure 3), which results from the large sediment inputs typical of braided streams.

The trends in armour ratios with channel morphology documented here suggest that planform style, dominant macrobedforms, streambed mobility and grain size adjust together to dominant sediment supply conditions. In this regard, a typical sequence of reach types observed in many mountain basins corresponds to a downstream progression from step pool at headwaters, plane-bed (or forced pool-riffle) to pool-riffle and/or multithreaded channel morphologies at the piedmont valley (e.g. Warburton, 2007). In their seminal paper, Montgomery and Buffington (1997) suggested that this kind of longitudinal sequence describes opposing trends between sediment supply and transport capacities in the downstream direction. In this regard, Pitlick et al. (2008) documented a downstream trend to lower armour ratios in rivers from Colorado and Utah. The trends observed here are in good agreement with this general scheme.

Additionally, gravel-bed rivers exhibit a wide diversity of bed features that are larger than individual clasts and smaller than reach-scale patterns. Sediment supply plays a critical role in the development of one kind of bed structuration or another (Buffington and Montgomery, 1999; Venditti et al., 2017.). Dominant bedforms in gravel bed rivers evolve from gravel dunes (Carling, 1999) and bedload sheets in poorly armoured streams (Whiting et al., 1988; Nelson et al., 2009; Recking et al., 2009), to a sequence of pebble clusters (Brayshaw, 1984), transverse ribs (Koster, 1978; Allen, 1984), stone lines (Laronne and Carson, 1976) and reticulate stone cells (Church et al., 1998; Hassan and Church, 2000) with decreasing sediment supplies (Venditti et al., 2017). Indeed, the stability of a gravel streambed is increased by the presence of particle arrangements and clusters (e.g., Reid and Frostick, 1984; Church et al., 1998; Hassan and Church, 2000; Piedra et al., 2012; Ockelford and Haynes, 2013; Heays et al., 2014). Therefore, streambed textures adjust to sediment supply reductions not only through surface coarsening, but also through a decrease in streambed mobility and a different bed surface organization. Venditti et al. (2017) have proposed a phase diagram for bedforms in gravel bed rivers, relating q^* to the armour ratio (Figures 16.5 and 16.9 in Venditti et al., 2017) that is in some way comparable to our Figure 7. If armour ratio varies in parallel to channel morphology, dominant macroforms, bed sediment mobility and streambed structures (as our analysis shows), then the armour ratio should be considered not only as some kind of 'textural imprint' of sediment supply conditions, but also as a proxy of the streambed's organization and structuration (Venditti et al., 2017).

6. Concluding Remarks

A large body of research in fluvial geomorphology has contributed to establishing the general idea that sediment supply, bedload fluxes, channel morphology, bankfull shear stresses and surface grain size are intimately related in gravel bed rivers. In this paper, we aimed to quantify the existing links between sediment supply and surface coarsening. Based on the re-analysis of a large database of bedload discharge information for gravel-bed streams, we have proposed semi-empirical relations describing how surface grain-size and armour ratios evolve with the balances between bedload yields and channel sediment transport capacities. Armour ratios increase with decreasing sediment inputs, as inferred from the dimensional analysis of bedload equations and as already shown by previous flume experiments.

Accounting for armouring is important for many reasons, since it influences the local availability of bedload, hydraulic roughness, bed permeability, and physical conditions for aquatic organisms. We believe that the empirical relationships found here between bedload yields and armour ratios have the potential to provide a quantitative frame for exploring the links between surface armouring, hydraulics and sediment availability in specific gravel-bed reaches and are a step towards predicting textural adjustments to changes in sediment supply (for example, downstream dams). Additionally, since armouring can provide important qualitative information about the bedload regime (e.g. partial mobility vs. full mobility, sediment supply) of a specific river reach, our results may potentially provide some interesting clues for palaeohydrological analysis.

Acknowledgements: The present work has been possible thanks to the financial support provided by the grant ACB17-44, co-funded by the post-doctoral 'Clarín' program-FICYT (Government of the Principality of Asturias) and the Marie Curie Co-Fund. This work was also performed within the framework of the EUR H2O'Lyon (ANR-17-EURE-0018) of Université de Lyon (UdL), within the program 'Investissements d'Avenir' operated by the French National Research Agency (ANR). We would like to thank Pablo Turrero García and Daniel Grace for their review of the English version of the manuscript.

Notations

D:	Grain-size (particle diameter)
D_{is}:	*i*-th percentile of the surface grain-size distribution
D_{iss}:	*i*-th percentile of the subsurface grain-size distribution
D_i^*:	Armour ratio, or the ratio between the *i*-the percentiles of the surface and subsurface grain-size distributions
D_i^{**}:	Corrected version of the armour ratio, i.e. armour ratio computed accounting for the inherent covariation between surface and subsurface grain sizes
f:	Ratio between the armour ratio estimated based on the 84-th percentiles (D_{84}) and the armour ratio based on the median size (D50) of the grain size distribution
GSD:	Grain size distribution
ϕ:	Bedload transport intensity (Einstein parameter)
q_s:	Bedload transport rate per unit width
q_{ss}:	Channel's bedload transport capacity (per unit width) to mobilize the subarmour sediment
q_{sss}:	Channel's bedload transport capacity (per unit width) to mobilize the subarmour sediment
q^*:	Bedload 'supply index', or the ratio between qss and qsss
Q:	Peak discharge
Q_d:	Peak discharge for the dominant discharge
Q/Q_d:	Flow ratio
ω:	Specific streampower
τ:	Section-averaged bed shear stress
τ^*:	Dimensionless (section-averaged) Shields shear stress
τ_c:	Critical (section averaged) bed shear stress for sediment entrainment
τ_{cs}:	Critical (section averaged) bed shear stress for the inception of motion of the surface sediment particles
τ_{css}:	Critical (section averaged) bed shear stress for the inception of motion of the subsurface sediment particles
τ_{ci}^*:	Critical threshold Shields stress for entrainment particle with sizes corresponding to the *i*-th percentile of the grain-size distribution

References

Allen, J. R. L. (1984). *Sedimentary Structures, Their Character and Physical Basis*. Elsevier, Amsterdam.

Almedeij, J. H. (2002). *Bedload transport in gravel- bed streams under a wide range of Shields stresses*. Ph.D. thesis, Va. Polytech. Inst. and State Univ., Blacksburg.

Andrews, E. D. (1994). Marginal bed load transport in a gravel bed stream, Sagehen Creek, California. *Water Resources Research*, 30, 2241–2250.

Andrews, E. D. and Erman, D. C. (1986). Persistence in the size distribution of surficial bed material during an extreme snowmelt flood. *Water Resources Research*, 22, 191–197.

Andrews, E.D. and Parker, G. (1987): Formation of a coarse surface layer as the response to gravel mobility. In: Thorne, C.R., Bathurst, J.C. and Hey, R.D. (eds). *Sediment transport in gravel-bed rivers*, pp. 269-300. Chichester: Wiley.

Bacchi, V., Recking, A., Eckert, N., Frey, P., Piton, G. and Naaim, M. (2014). The effects of kinetic sorting on sediment mobility on steep slopes. *Earth Surface Processes and Landforms*, 39, 1075–1086.

Barry, J. J., Buffington, J. M. and King, J. G. (2004). A general power equation for predicting bedload transport rates in gravel bed rivers. *Water Resources Research*, 40, W104001.

Berni, C., Perret, E. and Camenen, B. (2018). Characteristic time of sediment transport decrease in static armour formation. *Geomorphology*, 317, 1-9.

Bertin, S. and Friedrich, H. (2018). Effects of surface texture and structure on the development of stable fluvial armors. *Geomorphology*, 306, 64-79.

Borland, W. M. (1960). *Stream Channel Stability*. U.S. Bureau of Reclamation, Denver.

Brasington, J., Vericat, D. and Rychov, I. (2012). Modeling river bed morphology, roughness, and surface sedimentology using high resolution terrestrial laser scanning. *Water Resources Research*, 48 (2012), Article W11519.

Brayshaw, A. C. (1984). Characteristics and origin of cluster bedforms in coarse-grained alluvial channels. *Sedimentology of Gravels and Conglomerates*, 10, 77-85.

Buffington, J. M. (2012). Changes in channel morphology over human time scales. In: Church, M., Biron, P.M., Roy, A.G. (eds.), *Gravel-bed Rivers: Processes, Tools, Environments*, chapter 32, pp. 435–463. Wiley, Chichester, UK.

Buffington, J. M. and Montgomery, D. R. (1999). A procedure for classifying textural facies in gravel-bed rivers. *Water Resources Research*, 35 (6), 1903-1914.

Bunte, K. and Abt, S. R. (2001). *Sampling surface and subsurface particle-size distributions in wadable gravel-and cobble-bed streams for analyses in sediment transport, hydraulics, and streambed monitoring*. Gen. Tech. Rep. RMRS-GTR-74. Fort Collins,CO: U.S. Department of Agriculture, Forest Service, Rocky Mountain Research Station. 428 p.

Buscombe, D. (2008). Estimation of grain size distributions and associated parameters from digital images of sediment. *Sedimentary Geology*, 210, 1-10.

Butler, J. B., Lane, S. N. and Chandler, J. H. (2001). Automated extraction of grain-size data for gravel surfaces using digital image processing. *Journal of Hydraulic Research*, 39, 519-529.

Camenen, B., Holubová. K., Lukac, M., Le Coz, J. and Paquier, A. (2011). Assessment of Methods Used in 1D Models for Computing Bed-Load Transport in a Large River: The Danube River in Slovakia. *Journal of Hydraulic Engineering*, 137 (10).

Carling, P. A. (1999). Subaqueous gravel dunes. *Journal of Sedimentary Research*, 69, 534– 545.

Chin, C. O., Melville, B. W. and Raudkivi, A. J. (1994). Streambed armouring. *Journal of Hydraulic Engineering*, 120 (8).

Chin, A. and Wohl, E. (2005). Toward a theory for step pool in stream channels. *Progress in Physical Geography*, 29, 275– 296.

Church, M. (2006). Bed material transport and the morphology of alluvial river channels. *Annual Review of Earth and Planetary Sciences*, 34 (1), 325-354.

Church, M. and Hassan, M. A. (2002). Mobility of bed material in Harris Creek. *Water Resources Research*, 38 (11), 1237.

Church, M. and Hassan, M. (2005). Upland gravel-bed rivers with low sediment transport. In: Garcia, C. and Batalla, R.J. (eds). *Catchment Dynamics and River Processes. Mediterranean and Other Climate Regions.* Developments in Earth Surface Processes 7, pp. 141-168, Amsterdam, Elsevier.

Church, M., Hassan, M. A. and Wolcott, J. F. (1998). Stabilizing self- organized structures in gravel- bed stream channels: Field and experimental observations. *Water Resources Research*, 34 (11), 3169– 3179.

Church, M. A., McLean, D. G. and Wolcott, J. F. (1987). River Bed Gravels: Sampling and Analysis. In: Thorne, C. R., Bathurst, J. C. and Hey, R. D. (eds). S*ediments transport in Gravel Bed Rivers*, pp. 43-88. John Wiley and Sons, New York.

Church, M. and Rood, K. (1983). *Catalogue of alluvial river channel regime data*, Dep. of Geography, Univ. of British Columbia, Vancouver.

Church, M. and Zimmermann, A. (2007). Form and stability of step- pool channels: research progress. *Water Resources Research*, 43, W03415.

Clayton, J. A. and Pitlick, J. (2008). Persistence of the surface texture of a gravel-bed river during a large flood. *Earth Surface Processes and Landforms*, 33, 661–673.

Cui, Y., Parker, G., Lisle, T. E., Gott, J., Hansler- Ball, M. E., Pizzuto, J. E., Allmendinger, N. E., and Reed, J. M. (2003). Sediment pulses in mountain rivers: 1. Experiments. *Water Resources Research*, 39, 1239,

Curran, J. and Waters, K. A. (2014). The importance of bed sediment sand content for the structure of a static armor layer in a gravel bed river. *Journal of Geophysical Research: Earth Surface*, 119, 1484–1497.

Dietrich, W., Kirchner, J., Ikeda, H., and Iseya, F. (1989). Sediment supply and the development of the coarse surface layer in gravel-bedded rivers. *Nature*, 340, 215–217.

Emmett, W. W. and H. R. Seitz (1974). *Suspended- and bedload- sediment transport in the Snake and Clearwater rivers in the vicinity of Lewiston, Idaho (July 1973 through July 1974)*. U.S. Geological Survey, Boise, Idaho.

Erwin, S. O., Schmidt, J. C. and Nelson, N. C. (2011). Downstream effects of impounding a natural lake: the Snake River downstream from Jackson Lake Dam, Wyoming, USA. *Earth Surface Processes and Landforms*, 36, 1421-1434.

Ferdowsi, B., Ortiz, C.P., Houssais, M. and Jerolmack, D.J. (2017). River-bed armouring as a granular segregation phenomenon. *Nature Communications*, 8, 1363.

Ferguson, R.I. (2003). The missing dimension: effects of lateral variation on 1-D calculations of fluvial bedload transport. *Geomorphology*, 56, 1-14.

Ferguson, R. (2007). Flow resistance equations for gravel and boulder bed streams. *Water Resources Research*, 43, W05427, 1– 12.

Ferguson, R., and Church, M. (2009). A critical perspective on 1-D modeling of river processes: gravel load and aggradation in lower Fraser River. *Water Resources Research*, 45, W11424

Francalanci, S., Solari, L., Toffolon, M. and Parker G. (2012). Do alternate bars affect sediment transport and flow resistance in gravel- bed rivers? *Earth Surface Processes and Landforms*, 37 (8), 866– 875.

Gessler, J., (1967). *The Beginning of Bedload Movement of Mixtures Investigated as Natural Armoring in Channels*. W.M. Keck Laboratory of Hydraulics and Water Resources, California Institute of Technology, Pasadena, Translation T-5.

Gessler, J. (1970). Self- stabilizing tendencies of alluvial channels. *Journal of the Waterways, Harbors and Coastal Engineering Division, American Society of Civil Engineers*, 96 (2), 235– 249, 1970.

Gomez, B. (1983). Temporal variations in bedload transport rates: the effect of progressive bed armouring. *Earth Surface Processes and Landforms*, 8 (1), 41–54.

Gomez, B. (1988). *Two data sets describing channel- wide temporal variations in bedload-transport rates*. U.S. Geological Survey. Public Data File, 88- 88, 26 pp.

Gomez, B. (1993). Roughness of stable, armored gravel beds. *Water Resources Research*, 29 (11), 3631–3642.

Gomez, B. (1994). Effects of particle shape and mobility on stable armor development. *Water Resources Research*, 30 (7), 2229–2239.

Graham, D. J., Reid, I. and Rice, S. P. (2005). Automated sizing of coarse-grained sediments: image-processing procedures. *Mathematical Geology*, 37, 1-28.

Harrison, H. S. (1950). *Report on special investigations of bed sediment segregation in a degrading bed*. Inst. of Eng. Res., University of California, Berkeley.

Haschenburger, J.K. and Wilcock, P.R. (2003). Partial transport in a natural gravel bed channel. *Water Resources Research*, 39 (1), 1020.

Haschenburger, J. K. (2017) Streambed Disturbance over a Long Flood Series. *River Research and Applications*, 33: 753– 765.

Hassan, M. A. and M. Church (2000). Experiments on surface structure and partial sediment transport. *Water Resources Research*, 36, 1885 – 1895.

Hassan, M. A., Egozi, R. and Parker, G. (2006). Experiments on the effect of hydrograph characteristics on vertical grain sorting in gravel bed rivers. *Water Resources Research*, 42, W09408.

Hassan, M. A. and Zimmermann, A. (2012). Channel Response and Recovery to Changes in Sediment Supply. In: Church, M., Biron, P. M. and Roy, A. G. (eds). *Gravel-Bed Rivers: Processes, Tools, Environments*, chapter 33, pp. 464-473. Wiley & Sons, Chichester, UK.

Heays, K. G., Friedrich, H. and Melville, B. W. (2014). Laboratory study of gravel-bed cluster formation and disintegration. *Water Resources Research*, 50, 2227–2241.

Heritage, G. and Milan, D. J. (2009). Terrestrial laser scanning of grain roughness in a gravel bed river. *Geomorphology*, 113 (1), pp. 4-11.

Hinton, D., Hotchkiss, R. H. and Cope, M. (2018). Comparison of Calibrated Empirical and Semi-Empirical Methods for Bedload Transport Rate Prediction in Gravel Bed Streams. *Journal of Hydraulic Engineering*, 144 (7).

Ibbeken, H. and Schleyer, R. (1986). Photo‐ sieving: A method for grain‐ size analysis of coarse-grained, unconsolidated bedding surfaces. *Earth Surface Processes and Landforms*, 11, 59-77.

Jain, S. (1990). Armor or Pavement. *Journal Hydraulic Engineering. ASCE*, 116, 436– 440.

Jones, M. L. and H. R. Seitz (1980). *Sediment transport in the Snake and Clearwater rivers in the vicinity of Lewiston, Idaho*. U.S. Geological Survey. Open File Rep., 80‐ 690, 179 pp.

Kellerhals, R. and Bray, D.L. (1971). Sampling procedures for coarse fluvial sediment. *Journal of the Hydraulic Division. ASCE*, 97. 1165-1179.

King, J. G., W. W. Emmett, P. J. Whiting, R. P. Kenworthy, and J. J. Barry (2004). *Sediment transport data and related information for selected gravel-bed streams and rivers in Idaho*. U.S. For. Serv. Gen. Tech. Rep. RM, RMRS-GTR-131, 26 pp.

Klaassen, G. J. (1988). Armoured river beds during flood. *Tech. Rep. 394, Delft Hydraulics, Emmeloord, the Netherlands*.

Koster, E. H. (1978). Transverse ribs: their characteristics, origin, paleohydraulic significance. In: Miall, A. D. (ed). *Fluvial Sedimentology*, pp. 161-186. Canadian Society of Petroleum Geologists. Mem. 5.

Kuhnle, R. A. (1992). Fractional transport rates of bedload on Goodwin Creek. In: Billi, P. (ed). Dynamics of Gravel Bed Rivers, pp. 141–155, John Wiley, New York.

Kuhnle, R.A. and Willis, J. C. (1992). Mean size distribution of bed load on Goodwin Creek. *Journal of Hydraulic Engineering*, 118, 1443–1446.

Lamarre, H. and Roy, A. G. (2008). The role of morphology on the displacement of particles in a step–pool river system. *Geomorphology*, 99, 270– 279.

Lane, E.W. (1955). Design of stable channels, *Transactions ASCE*, Paper no. 2776, 20, 1234-1279.

Laronne, J.B. and Carson, M.A. (1976). Interrelationships between bed morphology and bed material transport for a small, gravel-bed channel. *Sedimentology*, 23 (1), 67–85.

Laronne, J. B and Reid, I. (1993). Very high rates of bedload sediment transport by ephemeral desert rivers. *Nature*, 366, 148-150.

Laronne, J. B., Reid, I., Yitshack, Y. and Frostick, L. E. (1994). The non-layering of gravel streambeds under ephemeral flood regimes. *Journal of Hydrology*, 159 (1-4), 353-363.

Lindeman, R.H., Merenda, P.F. and Gold, R.Z. (1980). *Introduction to Bivariate and Multivariate Analysis*, Scott Foresman & Co: Glenview, IL, USA.

Lisle, T. E. (1986). Stabilization of a gravel channel by large streamside obstruction and bedrock bends, Jacoby Creek, northwestern California. *Geological Society of American Bulletin*, 97, 999–1011.

Lisle, T. E. (1989). Sediment transport and resulting deposition in spawning gravels, north coastal California. *Water Resources Research*, 25, 1303–1319.

Lisle, T.E. (1995). Particle size variations between bed load and bed material in natural gravel bed channels. *Water Resources Research*, 31, 1107–1118.

Lisle, T. E. and Hilton, T. (1992). The volume of fine sediment in pools: an index of sediment supply in gravel- bed streams. *Water Resources Bulletin*, 28 (2), 371– 383.

Lisle, T. E. and Madej, M. A. (1992). Spatial variation in armouring in a channel with high sediment supply. In: Billi, P., Hey, R. D., Thorne, C.R. and Tacconi, P. (ed). *Dynamics of Gravel-bed Rivers,* pp. 277-293*,* John Wiley and Sons.

Little, W. C., and Mayer, P. G. (1972). *The role of sediment gradation of channel armoring*. Publ. ERC- 0672, 104 pp., Ga. Inst. of Technol.

MacKenzie, L. G., Eaton, B. C. and Church, M. (2018). Breaking from the average: Why large grains matter in gravel- bed streams. *Earth Surface Processes and Landforms*, 43, 3190–3196.

Madej, M. A. and V. Ozaki (1996). Channel response to sediment wave propagation and movement, Redwood Creek, California, USA. *Earth Surface Processes and Landforms*, 21, 911 – 927.

Mao, L. (2012). The effect of hydrographs on bed load transport and bed sediment spatial arrangement. *Journal of Geophysical Research: Earth Surface,* 117 (F3).

Mao, L., Cooper, J. R., and Frostick, L. E. (2011). Grain size and topographical differences between static and mobile armour layers. *Earth Surface Processes and Landforms*, 36, 1321–1334.

Marion, A. and Fraccarollo, L. (1997). Experimental investigation of mobile armoring development. *Water Resources Research*, 33, 1447–1453.

McLean, D. G., Church, M. and Tassone, B. (1999). Sediment transport along lower Fraser River: 1. Measurements and hydraulic computations. *Water Resources Research*, 35, 2533–2548.

Marion, A., Tait, S.J. and McEwan, I.K. (2003). Analysis of small-scale gravel bed topography during armoring. *Water Resources Research*, 39 (12).

Métivier, F. and Barrier, L. (2012). Alluvial landscape evolution: what do we know about metamorphosis of gravel bed meandering and braided streams? In: Church, M., Biron, P., and Roy, A. (eds). Gravel-bed Rivers: processes, tools, environments, chapter 34, 474-501. Wiley & Sons, Chichester.

Métivier, F., Lajeunesse, E. and Devauchelle, O. (2017). Laboratory rivers: Lacey's law, threshold theory, and channel stability. *Earth Surface Dynamics*, 5, 187–198.

Meyer-Peter, E. and Muller, R. (1948). Formulas for Bed Load Transport. *Proceedings of 2nd meeting of the International Association for Hydraulic Structures Research*, Delft, 7 June 1948, 39-64.

Milhous, R. T. (1973). *Sediment transport in a gravel- bottomed stream*. Ph.D. thesis, Oregon State University, Corvallis.

Misset, C., Recking, A., Legout, C., Bakker, M., Bodereau, N., Borgniet, L., Cassel, M., Geay, T., Gimbert, F., Navratil, O., Piegay, H., Valsangkar, N., Cazilhac, M., Poirel, A. and Zanker, S. (in press). Combining multi-physical measurements to quantify bedload transport and morphodynamic interactions in an alpine braiding river reach. *Geomorphology*.

Montgomery, D.R. and Buffington, J.M. (1997). Channel-reach morphology in mountain drainage basins. *Geological Society of America Bulletin*, 109, 596–611.

Moog, D. B. and Whiting, P. J. (1998). Annual hysteresis in bed load rating curves. *Water Resources Research*, 34 (9), 2393– 2399.

Mueller, E. R. and Pitlick, J. (2005). Morphologically based model of bed load transport capacity in a headwater stream. *Journal of Geophysical Research*, 110, F02016.

Mueller, E. R. and Pitlick, J. (2014). Sediment supply and channel morphology in mountain river systems: 2. Single thread to braided transitions. *Journal of Geophysical Research: Earth Surface*, 119, 1516– 1541.

Mueller, E. R., Pitlick, J. and Nelson, J. M. (2005). Variation in the reference Shields stress for bed load transport in gravel- bed streams and rivers. *Water Resources Research*, 41, W04006.

Muskatirovic, J. (2008). Analysis of bedload transport characteristics of Idaho streams and rivers. *Earth Surface Processes and Landforms*, 33, 1757–1768.

Nelson, P. A., Dietrich, W. E. and Venditti, J. G. (2010). Bed topography and the development of forced bed surface patches. *Journal of Geophysical Research*, 115.

Nelson, P. A., Venditti, J. G., Dietrich, W. E., Kirchner, J. W., Ikeda, H., Iseya, F., and Sklar, L. S. (2009), Response of bed surface patchiness to reductions in sediment supply. *Journal of Geophysical Research*, 114, F02005.

Ockelford A. and Haynes, H. (2013). The impact of stress history on bed structure. *Earth Surface Processes and Landforms*, 38 (7), 717– 727.

Orrú, C., Blom, A. and Uijttewaal W.S. J. (2016). Armor breakup and reformation in a degradational laboratory experiment. *Earth Surface Dynamics*, 4, 461-470.

Paola, C. (1989). Topographic sorting. *Eos. Transactions American Geophysical Union*, 70, 332.

Parker, G. (1978). Self- formed rivers with equilibrium banks and mobile bed: Part II. The gravel river. *Journal of Fluid Mechanics*, 89 (1), 127– 148, 1978.

Parker, G. (1979). Hydraulic geometry of active gravel rivers. *Journal of the Hydraulics Division. American Society of Civil Engineers*, 105 (HY9), 1185– 1201, 1979.

Parker, G. (2004). *1D Sediment Transport Morphodynamics with Applications to Rivers and Turbidity Currents*. Copyrighted ebook, available at: http://hydrolab.illinois.edu/people/parkerg//morphodynamics_e-book.htm.

Parker, G. (2008). Transport of Gravel and Sediment Mixtures. In: García, M. (ed). *Sedimentation Engineering: Processes, Measurements, Modeling, and Practice.* Manual and Reports in Engineering Practice No. 110, American Society of Civil Engineers: Reston, VA, 165-264.

Parker, G. and Klingeman, P.C. (1982). On why gravel bed streams are paved. *Water Resources Research*, 18 (5), 1409–1423.

Parker, G., Klingeman, P.C. and McLean, D.C. (1982). Bedload and size distribution in paved, gravel-bed streams. *Proceedings of the American Society of Civil Engineers, Journal of the Hydraulics Divisio*n, 108, 544-571.

Parker, G. and Sutherland, A.J. (1990). Fluvial armor. *Journal of Hydraulic Research*, 28 (5), 529–544.

Parker, G., and C. M. Toro-Escobar (2002). Equal mobility of gravel in streams: The remains of the day. *Water Resources Research*, 38(11), 1264.

Parker, G., Wilcock, P. R., Paola, C., Dietrich, W. E. and Pitlick, J. (2007). Physical basis for quasi- universal relations describing bankfull hydraulic geometry of single- thread gravel bed rivers. *Journal of Geophysical Research*, 112, F04005.

Pfeiffer, A. M. and Finnegan, N. J. (2018). Regional variation in gravel riverbed mobility, controlled by hydrologic regime and sediment supply. *Geophysical Research Letters*, 45, 3097– 3106.

Pfeiffer, A. M., Finnegan, N. J. and Willenbring, J. K. (2017). Sediment supply controls gravel river geometry. *Proceedings of the National Academy of Sciences*, 114 (13), 3346-3351.

Phillips, C. B., Hill, K. M., Paola, C., Singer, M. B. and Jerolmack, D. J. (2018). Effect of flood hydrograph duration, magnitude, and shape on bed load transport dynamics. *Geophysical Research Letters*, 45, 8264– 8271.

Phillips, C. B. and Jerolmack, D. J. (2016). Self-organization of river channels as a critical filter on climate signals. *Science*, 352 (6286), 694-697.

Piedra, M. M., Haynes, H. and Hoey, T. B. (2012). The spatial distribution of coarse surface grains and the stability of gravel river beds. *Sedimentology*, 59, 1014–1029.

Pitlick, J., Mueller, E. R. and Segura, C. (2012). Differences in sediment supply to braided and single- thread channels: what do the data tell us? In: Church, M., Biron, P. M. and Roy, A. G. (eds). *Gravel- Bed Rivers: Processes, Tools, Environments*, chapter 35, pp. 502-511. Wiley & sons, Chichester, U. K.

Pitlick, J., Mueller, E. R., Segura, C., Cress, R. and Torizzo, M. (2008). Relation between flow, surface layer armoring and sediment transport in gravel bed rivers. *Earth Surface Processes and Landforms*, 33, 1192–1209.

Piton, G. and Recking, A. (2017). The concept of travelling bedload and its consequences for bedload computation in mountain streams. *Earth Surface Processes and Landforms*, 42, 1505– 1519.

Powell, D. M., Reid, I. and Laronne, J. B. (2001). Evolution of bed load grain size distribution with increasing flow strength and the effect of flow duration on the caliber of bed load sediment yield in ephemeral gravel bed rivers. *Water Resources Research*, 37 (5), 1463–1474.

Powell, D. M., Ockelford, A., Rice, S. P., Hillier, J. K., Nguyen, T., Reid, I., Tate, N. J. and Ackerley, D. (2016). Structural properties of mobile armors formed at different flow strengths in gravel- bed rivers. *Journal of Geophysical Research: Earth Surface*, 121, 1494– 1515.

Proffitt, G. T. and Sutherland, A. J. (1983). Transport of non uniform sediments. *Journal of Hydraulic Research*, 21(1), 33-43.

Recking, A. (2010). A comparison between flume and field bed load transport data and consequences for surface based bed load transport prediction. *Water Resources Research*, 46, W03518.

Recking, A. (2012). Influence of sediment supply on mountain streams bedload transport. *Geomorphology*, 175-176, 139-150.

Recking, A. (2013a). An analysis of nonlinearity effects on bed load transport prediction. *Journal of Geophysical Research: Earth Surface*, 118, 1264– 1281.

Recking, A. (2013b). Simple method for calculating reach-averaged bed-load transport. *Journal of Hydraulic Engineering*, 139 (1), 70–75.

Recking, A. (2016). A generalized threshold model for computing bed load grain size distribution. *Water Resources Research*, 52, 9274– 9289.

Recking, A., Leduc, P., Liébault, F. and Church, M. (2012). A field investigation of the influence of sediment supply on step- pool morphology and stability. *Geomorphology*, 139–140, 53– 66.

Recking, A., Piton, G., Vázquez- Tarrío, D. and Parker, G. (2016). Quantifying the morphological print of bedload transport. *Earth Surface Processes and Landforms*, 41(6), 809– 822.

Reid, I. and Frostick, L. E. (1984). Particle interaction and its effect on the thresholds of initial and final bedload motion in coarse alluvial channels. In: Koster, E. H. and Steel, R. J. (eds). *Sedimentology of Gravels and Conglomerates*, pp. 61-68. Canadian Society of Petroleum Geologists. Memoir 10.

Reid, I. and Frostick, L. E. (1986). Dynamics of bedload transport in Turkey Brook, a coarse-grained alluvial channel. *Earth Surface Processes and Landforms*, 11, 143– 155.

Reid, I. and Laronne, J. B. (1995). Bedload sediment transport in an ephemeral stream and a comparison with seasonal and perennial counterparts. *Water Resources Research*, 31, 773-781.

Reid, I., Laronne, J. B. and Powell, D. M. (1995). The Nahal Yatir bedload database: Sediment dynamics in a gravel- bed ephemeral stream. *Earth Surface Processes and Landforms*, 20, 845–857.

Rice, S. P. and Haschenburger, J. K. (2004). A hybrid method for size characterization of coarse subsurface fluvial sediments. *Earth Surface Processes and Landforms*, 29, 373-389.

Richards, K. and Clifford, N. (1991). Fluvial geomorphology: structured beds in gravelly rivers. *Progress in Physical Geography*, 15 (4), 407-411.

Rickenmann, D. and Recking, A. (2011). Evaluation of flow resistance in gravel- bed rivers through a large field data set. *Water Resources Research*, 47, W07538.

Rollet, A. J., Piégay, H., Dufour, S., Bornette, G., and Persat, H. (2014). Assessment of consequences of sediment deficit on a gravel river bed downstream of dams in restoration perspectives: application of a multicriteria, hierarchical and spatially explicit diagnosis. *River Research and Applications*, 30, 939– 953.

Ryan, S. E. and Emmett, W. W. (2002). *The nature of flow and sediment movement in Little Granite Creek near Bondurant, Wyoming*. Gen. Tech. Rep. RMRS-GTR-90. Ogden, UT. U.S. Department of Agriculture, Forest Service, Rocky Mountain Research Station. 48 p.

Ryan, S. E., Porth, L. S. and Troendle C. A. (2002). Defining phases of bedload transport using piecewise regression. *Earth Surface Processes and Landforms*, 27, 971–990.

Ryan, S. E., Porth, L. S. and Troendle, C. A. (2005). Coarse sediment transport in mountain streams in Colorado and Wyoming, USA. *Earth Surface Processes and Landforms*, 30, 269–288.

Rubin, D. M. (2004). A simple autocorrelation algorithm for determining grain size from digital images of sediment. *Journal of Sedimentary Research*, 74 (1), 160-165.

Segura, C., and Pitlick, J. (2015). Coupling fluvial- hydraulic models to predict gravel transport in spatially variable flows. *Journal of Geophysical Research: Earth Surface*, 120, 834–855.

Seitz, H. R. (1977). *Suspended- and bedload- sediment transport in the Snake and Clearwater rivers in the vicinity of Lewiston, Idaho (August 1975 through July 1976).* Boise, Idaho, U.S. Geological Survey, Open File Rep., 76- 886, 77 pp.

Sklar, L. S., Fadde, J., Venditti, J. G., Nelson, P., Wydzga, M. A., Cui, Y. and Dietrich, W. E. (2009). Translation and dispersion of sediment pulses in flume experiments simulating gravel augmentation below dams. *Water Resources Research*, 45, W08439.

Spiller, S., Rüther, N. and Baumann, B. (2012). Artificial reproduction of the surface structure in a gravel bed. *2nd IAHR Europe Congress*. TU München, Germany.

Turowski, J. M., Badoux, A. and Rickenmann, D. (2011). Start and end of bedload transport in gravel- bed streams. *Geophysical Research Letters*, 38, L04401.

Vázquez-Tarrío, D., Borgniet, L., Liébault, F. and Recking, A. (2017). Using UAS optical imagery and SfM photogrammetry to characterize the surface grain size of gravel bars in a braided river (Vénéon River, French Alps). *Geomorphology*, 285, 94-105.

Vázquez- Tarrío, D. and Menéndez- Duarte, R. (2015). Assessment of bedload equations using data obtained with tracers in two coarse- bed mountain streams (Narcea River basin, NW Spain). *Geomorphology*, 238, 78– 93.

Vázquez-Tarrío, D. and Batalla, R. J. (2019). Assessing Controls on the Displacement of Tracers in Gravel-Bed Rivers. *Water*, 11(8), 1598.

Vázquez- Tarrío, D., Recking, A., Liébault, F., Tal, M. and Menéndez- Duarte, R. (2019). Particle transport in gravel- bed rivers: Revisiting passive tracer data. *Earth Surface Processes and Landforms*, 44, 112– 128.

Vázquez-Tarrío, D., Tal, M., Camenen, B. and Piégay, H. (2019). Effects of continuous embankments and successive run-of-the-river dams on bedload transport capacities along the Rhône River, France. *Science of the Total Environment*, 658, 1375-1389.

Venditti, J. G., Dietrich, W. E., Nelson, P. A., Wydzga, M. A., Fadde, J. and Sklar, L. S. (2005). Can coarse surface layers in gravel- bedded rivers be mobilized by finer gravel bedload? *Eos Trans. AGU*, 86 (52), Fall Meet. Suppl., Abstract H51H- 05.

Venditti, J. G., Dietrich, W. E., Nelson, P. A., Wydzga, M. A., Fadde, J. and Sklar, L. S. (2010a). Mobilization of coarse surface layers in gravel-bedded rivers by finer gravel bed load. *Water Resources Research*, 46, W07506.

Venditti, J. G., Dietrich, W. E., Nelson, P. A., Wydzga, M. A., Fadde, J. and Sklar, L. S. (2010b). Effect of sediment pulse grain size on sediment transport rates and bed mobility in gravel bed rivers. *Journal of Geophysical Research: Earth surface*, 115, F03039.

Venditti, J. G., P. A. Nelson, R. W. Bradley, D. Haught, and A. B. Gitto (2017). Bedforms, structures, patches, and sediment supply in gravel- bed rivers. In: Tsutsumi, D. and Laronne, J. B. (ed). *Gravel- Bed Rivers: Processes and Disasters*, chapter 16, 439– 466. Wiley & Sons, Chichester, UK.

Vericat, D., Batalla, R. J. and Garcia, C. (2006). Breakup and reestablishment of the armour layer in a large gravel-bed river below dams: the lower Ebro. *Geomorphology*, 76, 122–136.

Wang, T. and Liu, X. (2009). The Breakup of Armor Layer in a Gravel Bed Stream with No Sediment Supply. In: Zhang, C. and Tang, H. (ed). *Advances in Water Resources and Hydraulic Engineering, Proceedings of 16th IAHR-APD Congress and 3rd Symposium of IAHR-ISHS*. Springer Berlin Heidelberg, 919–923.

Warburton, J. (2007). Mountain Environments. In: Perry, C. and Taylor, K. (eds). *Environmental Sedimentology*. Blackwell, Oxford.

Wathen S.J., Ferguson R.I., Hoey T.B. and Werritty A (1995). Unequal mobility of sand and gravel in weakly bimodal sediment. *Water Resources Research*, 31, 2087-2096.

Whiting, P. J., Dietrich, W. E., Leopold, L. B., Drake, T.G. and Shreve , R. L. (1988). Bedload sheets in heterogeneous sediment. *Geology*, 16, 105-108.

Wilcock, P. R. (2001). The flow, the bed, and the transport: interaction in flume and field. In: Mosley, P. (ed). *Proceedings of the Fifth Gravel-Bed Rivers Workshop*, pp. 183-219. New Zealand Hydrological Society, Wellington.

Wilcock, P. R. and Crowe, J. C. (2003). Surface-based models for mixed size sediment. *Journal of Hydraulic Engineering*, 129 (2).

Wilcock, P. R. and DeTemple, B. T. (2005). Persistence of armor layers in gravel-bed streams, *Geophysical Research Letters*, 32, L08402.

Wilcock, P. R. and Kenworthy, S. T. (2002). A two- fraction model for the transport of sand/gravel mixtures. *Water Resources Research*, 38(10), 1194.

Wilcock, P. R. and McArdell, B.W. (1993). Surface-based fractional transport rates: Mobilization thresholds and partial transport of a sand-gravel sediment. *Water Resources Research*, 29, 1297 – 1312.

Wilcock, P. R. and McArdell, B.W. (1997). Partial transport of a sand/gravel sediment. *Water Resources Research*, 33, 235 – 245.

Wilcock, P., Pitlick, J. and Cui, Y. (2009). *Sediment transport primer: estimating bed-material transport in gravel-bed rivers*. Gen. Tech. Rep. RMRS-GTR-226. Fort Collins, CO: U.S. Department of Agriculture, Forest Service, Rocky Mountain Research Station. 78 p.

Willets, B.B., Maizels, J.K. and Florence, J. (1988). The simulation of streambed armouring and its consequences. *Proceedings of the Institution of Civil Engineers*, 84 (3), 615–617.

Williams, G. P. and D. L. Rosgen (1989). *Measured total sediment loads (suspended loads and bedloads) for 93 United States streams.* U.S. Geological Survey. Open File Repport, 89-67, 128 pp.

Wolman, M. (1954). A method for sampling coarse river-bed material. *American Geophysical Union Transactions*, 35, 951–956, 1954.

Woodget, A. S. and Austrums, R. (2017). Subaerial gravel size measurement using topographic data derived from a UAV- SfM approach. *Earth Surface Processes and Landforms*, 42 (9), 1434– 1443.

Yager, E., Kenworthy, M., and Monsalve, A. (2015). Taking the river inside: Fundamental advances from laboratory experiments in measuring and understanding bedload transport processes. *Geomorphology*, 244, 21–32.

Yager, E. M., Venditti, J. G., Smith, H, J. and Schmeeckle, M. (2018). The trouble with shear stress. *Geomorphology*, 323, 41-50.

Zimmermann, A. and Church, M. (2001). Channel morphology, gradient profiles and bed stresses during flood in a step- pool channel. *Geomorphology*, 40, 311– 327.

Supplementary information to Vázquez-Tarrío et al. (*Textural signatures of sediment supply in gravel-bed rivers: re-visiting the armour ratio*)

S. 1. Computing section-averaged bed shear stresses for the compiled data

First, we used the available discharge information and Rickenmann and Recking's (2013) fit to Ferguson's (2007) friction law to estimate average flow velocity (U):

$$\frac{U}{\sqrt{g \cdot S \cdot D_{84}}} = 1.44 \cdot {q_l^*}^{0.6} \cdot \left[1 + \left(\frac{ql^*}{43.8}\right)^{0.82}\right]^{-0.24} \qquad \text{Eq. S1}$$

where g is the gravitational acceleration, S is the channel slope, D_{84} the 84th percentile of the surface GSD and q_l^* the dimensionless specific discharge:

$$ql^* = \frac{ql}{\sqrt{g \cdot S \cdot D_{84}^3}} \qquad \text{Eq. S2}$$

where q_l is the flow discharge normalized by channel width. Then, we estimated the water depth (d) from:

$$d = \frac{ql}{U} \qquad \text{Eq. S3}$$

For the hydraulic radius (R), we assumed a rectangular cross-section:

$$R = \frac{d \cdot w}{2 \cdot d + w} \qquad \text{Eq. S4}$$

where w is channel width. Finally, we computed the cross-section averaged basal shear stresses from the hydraulic radius-slope product:

$$\tau = \rho \cdot g \cdot R \cdot S \qquad \text{Eq. S5}$$

S. 2. A simple model for armour ratios based on bedload formulae

As explained in the main text, Dietrich et al. (1989) developed a metric (q^*) quantifying the balances between the sediment supplied into a reach and its actual bedload transport capacities (Dietrich et al., 1989; Montgomery and Buffington, 1997; Venditti et al., 2017):

$$q^* = \frac{q_{s_s}}{q_{s_{ss}}} \qquad \text{Eq. S6}$$

where q_s refers to the bedload transport rate per unit width and the subscripts s and ss to the surface and subsurface sediment, respectively. Combining eq. 1 with the Meyer-Peter and Muller's (1948) bedload transport equation, Dietrich et al. (1999) suggested:

$$q^* = \left[\frac{(\tau - \tau_{c_s})}{(\tau - \tau_{c_{ss}})}\right]^{1.5} \quad \text{Eq. S7}$$

where τ is the bed shear stresses and τ_c the critical stress for incipient motion. Writing shear stresses in their non-dimensional form (τ^*):

$$\tau^* = \frac{\tau}{(\rho_s - \rho) \cdot g \cdot D} \quad \text{Eq. S8}$$

Dietrich et al. (1989) finally arrived at:

$$q^* = \left(\frac{\frac{\tau}{\tau_{c_{ss}}} - \frac{D_{50_s}}{D_{50_{ss}}}}{{}^{\tau}/_{\tau_{c_{ss}}} - 1}\right)^{1.5} \quad \text{Eq. S9}$$

This expression quantifies the links between surface armouring (D_{50s}/D_{50ss}) and sediment supply (q^*), based on Meyer-Peter and Müller's bedload equation. The same reasoning could be applied to any other bedload equation. In this paper, we decided to use Recking's (2013b) equation (after Recking et al., 2016), since this equation has been tested and validated against bedload discharge information from natural gravel-bed rivers (e.g. Hinton et al., 2018). Recking (2013b) proposed the following expression for bedload rates:

$$\phi = A \cdot \frac{{\tau^*}^{\alpha}}{1 + \left(\frac{\tau_m^*}{\tau^*}\right)^{\beta}} \quad \text{Eq. S10}$$

where ϕ is the dimensionless transport rate, estimated using the Einstein parameter:

$$\phi = \frac{q_s}{\sqrt{g \cdot (s-1) \cdot D_{84}^3}} \quad \text{Eq. S11}$$

Coefficients A, α and β are three model parameters, for which values of 14, 2.5 and 4 were proposed, respectively (Recking, 2013b, Recking et al., 2016). τ^*_m is a mobility shear stress that allows to determine low transport conditions (with partial transport and bed clustering) apart from higher transport ones (Recking et al., 2016). Recking (2013b) estimates τ^*_m from:

$$\tau_m = (5 \cdot S + 0.06) \cdot \left(\frac{D_{84}}{D_{50}}\right)^{4.4 \cdot \sqrt{S} - 1.5} \qquad \text{Eq. S12}$$

Eq. S10 is such that for low transport conditions ($\tau^*_{ref} << \tau^*_m$):

$$\phi = A \cdot \frac{{\tau^*}^{\alpha+\beta}}{\tau_m^{\beta}} \qquad \text{Eq. S13}$$

and for higher transport conditions ($\tau^*_{ref} << \tau^*_m$):

$$\phi = {\tau^*}^{\alpha} \qquad \text{Eq. S14}$$

We can now combine equation S6 with the expression for the Einstein parameter (eq. S11):

$$q^* = \frac{q_{s_s}}{q_{s_{ss}}} = \frac{\phi_s}{\phi_{ss}} \cdot \left(\frac{D_{84ss}}{D_{84s}}\right)^{3/2} \qquad \text{Eq. S15}$$

Incorporating now eq. S13 into eq. S15, we can deduce:

$$q^* = \left(\frac{\tau^*_s}{\tau^*_{ss}}\right)^{\alpha+\beta} \cdot \left(\frac{\tau^*_{m_s}}{\tau^*_{m_{ss}}}\right)^{\beta} \cdot \left(\frac{D_{84_s}}{D_{84_{ss}}}\right)^{3/2} \qquad \text{Eq. S16}$$

for low transport conditions. Taking into account the expression for τ^*_m (eq. S12) and assuming a similar bed slope for the surface and subsurface case:

$$\frac{\tau^*_{m_s}}{\tau^*_{m_{ss}}} = \left(\frac{D_{84_s}}{D_{84_{ss}}}\right) \cdot \left(\frac{D_{50_{ss}}}{D_{50_s}}\right) \qquad \text{Eq. S17}$$

We could now introduce the idea that the armour ratio based on the D_{50} is linearly related to the value based on the D_{84} (see Figure 2 in the main text of the paper):

$$\left(\frac{D_{50_s}}{D_{50_{ss}}}\right) = f \cdot \left(\frac{D_{84_s}}{D_{84_{ss}}}\right) \qquad \text{Eq. S18}$$

Incorporating this idea into eq. S17, then:

$$\frac{\tau^*_{m_s}}{\tau^*_{m_{ss}}} = f \cdot \left(\frac{D_{84_s}}{D_{84_{ss}}}\right) \cdot \left(\frac{D_{84_s}}{D_{84_{ss}}}\right)^{-1} = f \qquad \text{Eq. S19}$$

Now, we can simplify eq. S16 based on eq. S19:

$$q^* = f \cdot \left(\frac{\tau^*_s}{\tau^*_{ss}}\right)^{\alpha+\beta} \cdot \left(\frac{D_{84_s}}{D_{84_{ss}}}\right)^{3/2} \qquad \text{Eq. S20}$$

Combining eq. S20 with that for the dimensionless Shields stress based on the D_{84} (eq. S8), then:

$$q^* = f \cdot \left(\frac{D_{84_s}}{D_{84_{ss}}}\right)^{3/2-\alpha-\beta} = f \cdot \left(\frac{D_{84_s}}{D_{84_{ss}}}\right)^{-5} \rightarrow \left(\frac{D_{84_s}}{D_{84_{ss}}}\right) = \frac{1}{f} \cdot {q^*}^{-1/5} \qquad \text{Eq. S21}$$

at low transport conditions.

At high transport conditions (when, $\tau^*_{ref} >> \tau^*_m$,), we should combine eq. S14 with eq. S15, and we arrive at:

$$q^* = \left(\frac{\tau^*_s}{\tau^*_{ss}}\right)^{\alpha} \cdot \left(\frac{D_{84_s}}{D_{84_{ss}}}\right)^{3/2} \qquad \text{Eq. S22}$$

Combining this expression with that for the dimensionless Shields stress:

$$q^* = \left(\frac{D_{84_s}}{D_{84_{ss}}}\right)^{3/2-\alpha} = \left(\frac{D_{84_s}}{D_{84_{ss}}}\right)^{-1} \rightarrow \left(\frac{D_{84_s}}{D_{84_{ss}}}\right) = {q^*}^{-1} \qquad \text{Eq. S23}$$

at full mobility conditions.

S. 3. How did we compute the 'bedload supply index' for the compiled dataset?

In Section 5 of the paper, we investigated and discussed whether available field measures of bedload fluxes may explain some trends in armour ratios (D^*) in the compiled data. More specifically, we analysed if the 'bedload supply index' (q^*) (at bankfull) could be correlated to the armour ratio in the available data and how well it adjusted to eq. S22 and/or S23 (as concluded in S. 2). According to Dietrich et al. (1989), q^* can be estimated from eq. S6. Estimating q^* from eq. S6 needs two inputs: i. actual bedload rates (in the numerator); and ii. bedload capacities in the denominator. In this paper, the numerator was defined from the bedload rates measured at (close to) dominant flows for each compiled study case. Bedload rates at dominant discharges were calculated following these steps: i. for each case study we defined the best power fit relating bedload to water discharge (based on the available bedload discharge information, see Table 1 in the paper); ii. we applied the obtained regression equation to the bankfull discharge, and we computed the bedload discharge at dominant flows. Concerning the denominator q_{ss} in eq. S6, we approached channel transport capacities (for all the selected case studies) from the bedload rates estimated using Recking's formula (eqs. S10-S11), but based on subsurface GSD.

The approach followed when defining $q*$ was obviously different in the case of flume data. As outlined in the main text of the paper, we also benefited from the results of some flume experiments that explored the role of sediment feed reductions on surface texture (Church et al., 1998; Church and Hassan, 2000; Nelson et al., 2009). Data from these flume experiments was extracted from the graphical reading of figures presented in Venditti et al. (2017). Venditti et al. (2017) estimated q^* for these flume experiments as the ratio between the bedload transport rate after the bed has adjusted to a new sediment feed divided by the transport rate for an unarmoured bed, before any feed reduction.

S. 4. How did we compute transport-stage ratios for the compiled dataset?

In Figures 8 and 10, we worked with and analysed transport stage ratios, which are defined as the ratio between Shields stresses and the critical (or reference) Shields stresses for incipient sediment motion (Wilcock et al., 2009):

$$Transport\ stage = \frac{\tau^*}{\tau_c^*} \qquad \text{Eq. S24}$$

Shields stresses are calculated for the 84th percentile of GSD in this paper, since D_{84} provides a measure of the largest grains in the bed, which probably control hydraulic roughness and morphological stability (MacKenzie et al., 2018). In eq. S24 (and Figures 8 and 10 in the paper), τ_c^* is the critical Shields stress below which no sediment transport is assumed to occur. This parameter is grain-size and slope dependent (Lamb et al., 2008; Pitlick et al., 2008; Recking, 2009). Here, we estimated it based on Recking (2009):

$$\tau_c^* = (1.32 \cdot S + 0.037) \cdot \left(\frac{D_{84}}{D_{50}}\right)^{-0.93} \qquad \text{Eq. S25}$$